UHECR Anisotropies: the experimental present with a glance to the past and a look at the future

Piera L. Ghia (IPN, Orsay, IN2P3/CNRS and Univ. Paris Sud and Paris Saclay)

Remembering Michael Hillas via his course on UHECRs at the ISAPP school 2005

UHECR Anisotropies: the experimental present with a glance at the past and a look at the future

Piera L. Ghia (IPN, Orsay, IN2P3/CNRS and Univ. Paris Sud and Paris Saclay)

Outline

1. Why bother with UHECRs anisotropies?
2. UHECR anisotropies: a glance at the past
3. Large-scale anisotropies at present
4. Small-scale anisotropies at present
5. UHECR anisotropies: a look at the future

Why bother with UHECR anisotropies?

Why bother with UHECR anisotropies?

A straightforward physics case

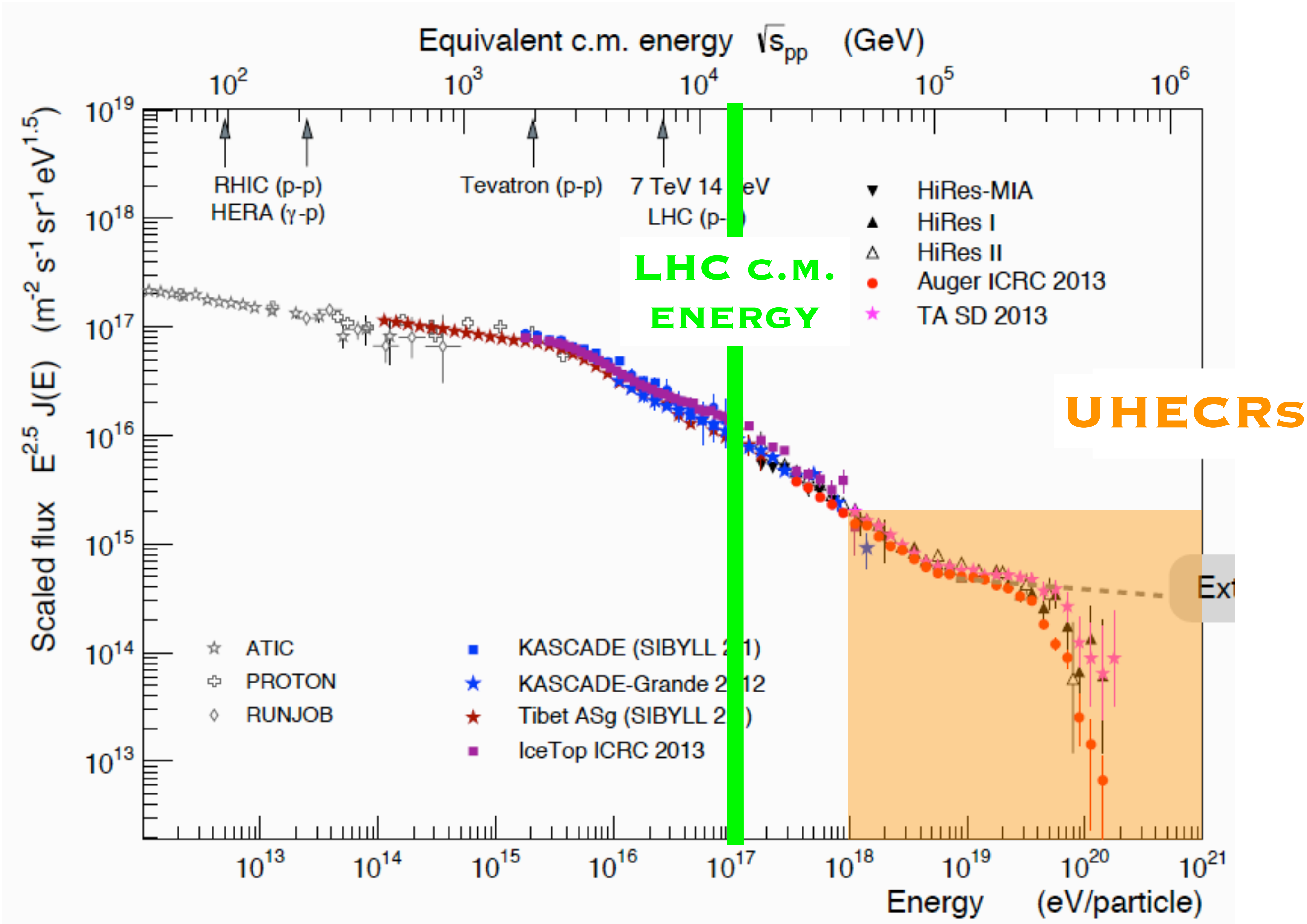

UHECRs exist and they are the Universe's highest-particles.
Some extraordinary processes are thus capable of accelerating them.

Why bother with UHECR anisotropies?

How far away do UHE CR originate?

Limits of Galactic trapping

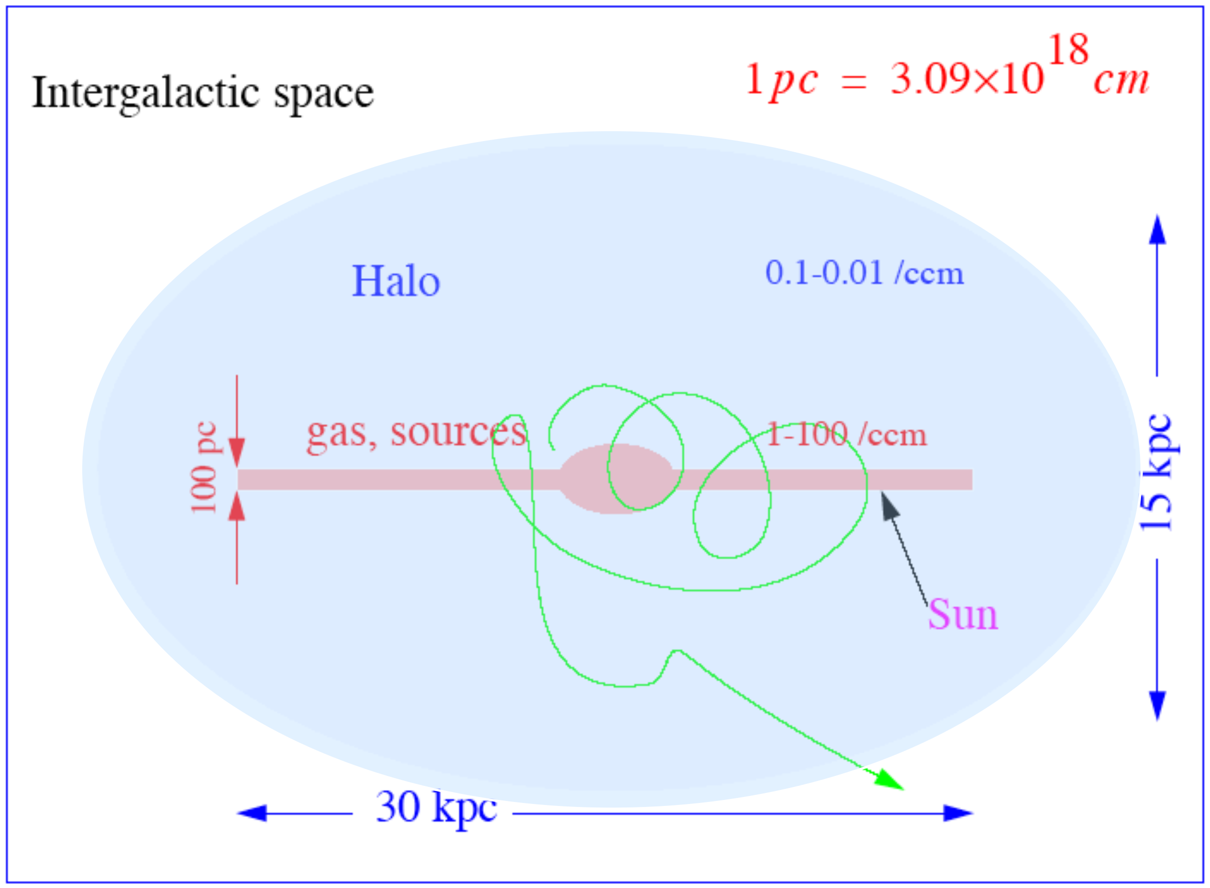

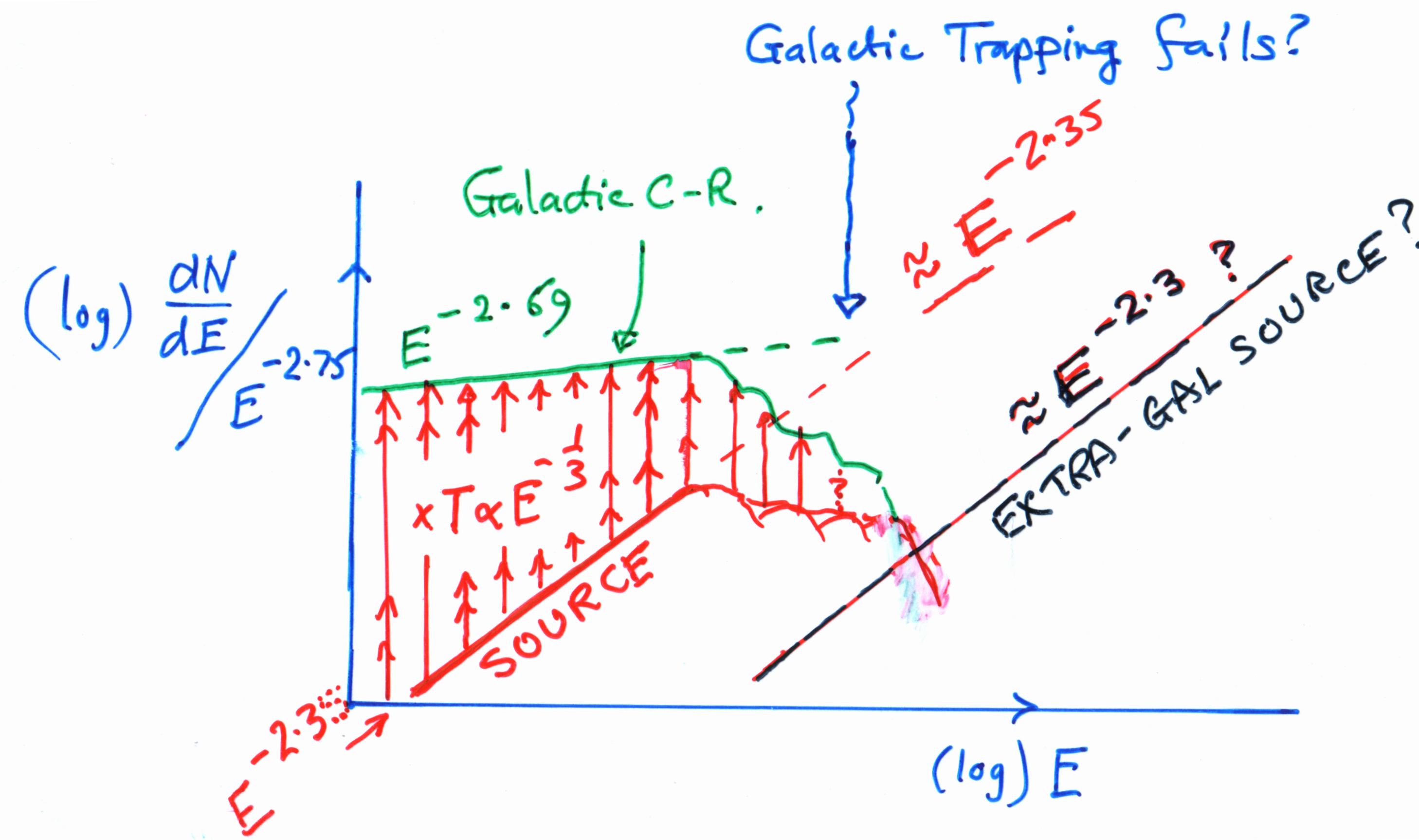

It appears that magnetic fields with Kolmogorov spectrum of turbulence are strong enough to produce diffusion with trapping lifetime $\propto E^{-1/3}$

Max^m? turbulence $\lambda \sim 100\,pc \approx r_{gyro}$ at $\sim 2\times10^{17}\,eV * Z$.

Above this — escape along field lines?

For cosmic rays above ≈ $10^{17\text{-}18}$ eV, the gyro-radius exceeds galactic dimensions for typical magnetic fields of O(μG) strength. Extra-galactic sources?

Why bother with UHECR anisotropies?

Absorption effects which give clue to distance

"GZK"

e^+e^-, π production, nuclear fragmentation

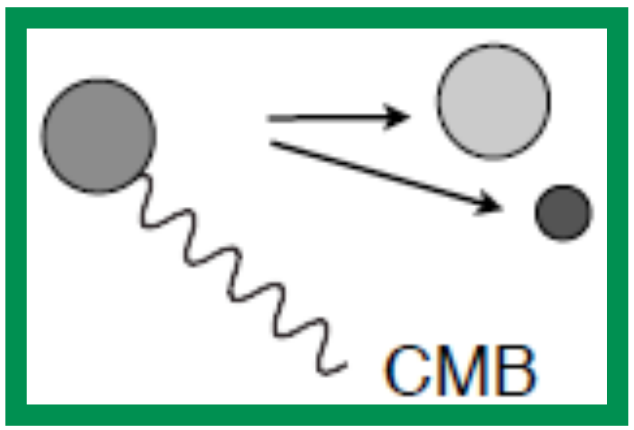

UHECRs interact with the extra-galactic photon backgrounds. For UHE protons the dominant reaction (above ≈ 5×10^{19} eV) is with the CMB, leading to the production of pions (photo-pion production)

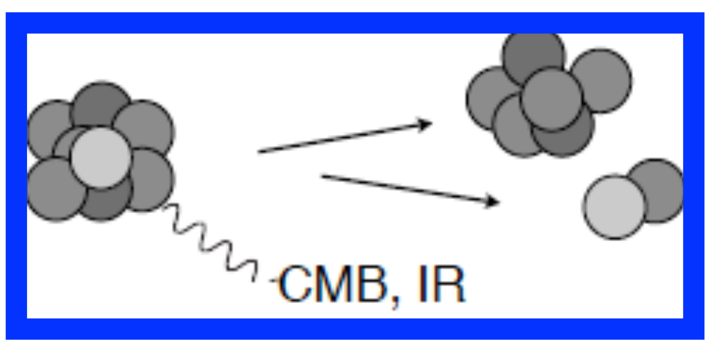

In case of UHE nuclei, the dominant interaction is with both CMB and infrared background. The resulting process of photo-dissociation leaves the nucleus with one or few less nucleons

The energy loss processes should limit the distance from which sources can contribute to the UHECR flux at Earth (≈ 200 Mpc* at ≈ 5×10^{19} eV)

* The"horizon" is of similar size for iron nuclei, and is smaller for intermediate-mass nuclei.

Why bother with UHECR anisotropies?

Where can we think of building an accelerator

Minimum size ~ $R_{gyro} / \beta_{plasma}$

→ few sites

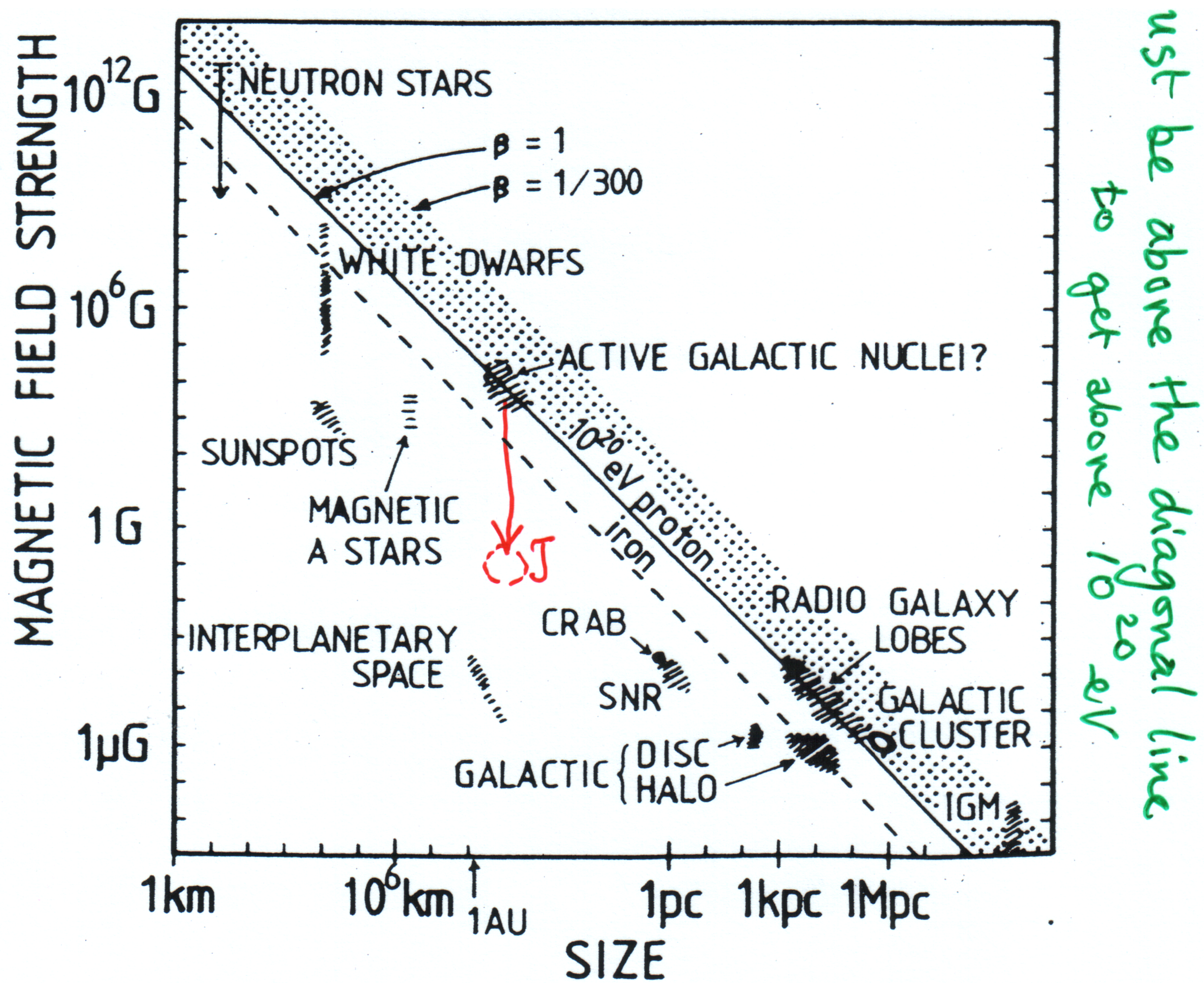

Only few, powerful, extragalactic sources can accelerate CRs to UHE

Why bother with UHECR anisotropies?

But paths not rectilinear

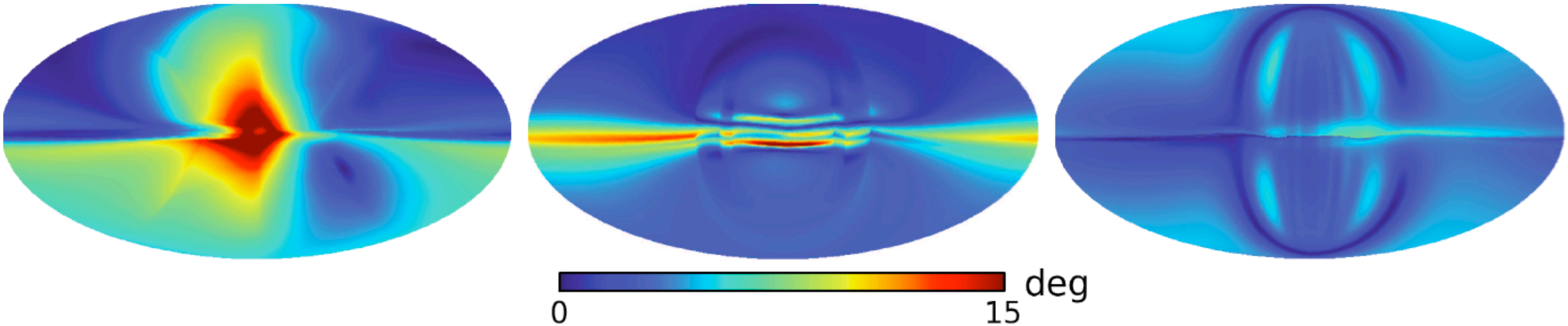

Jansson & Farrar 2012

Sun & Reich 2010

Pshirkov, Tinyakov & Kronberg 2011

Yet, the distribution of the arrival directions at the highest energies (rigidities) might show **small (intermediate) scale anisotropies**, reflective of their sources

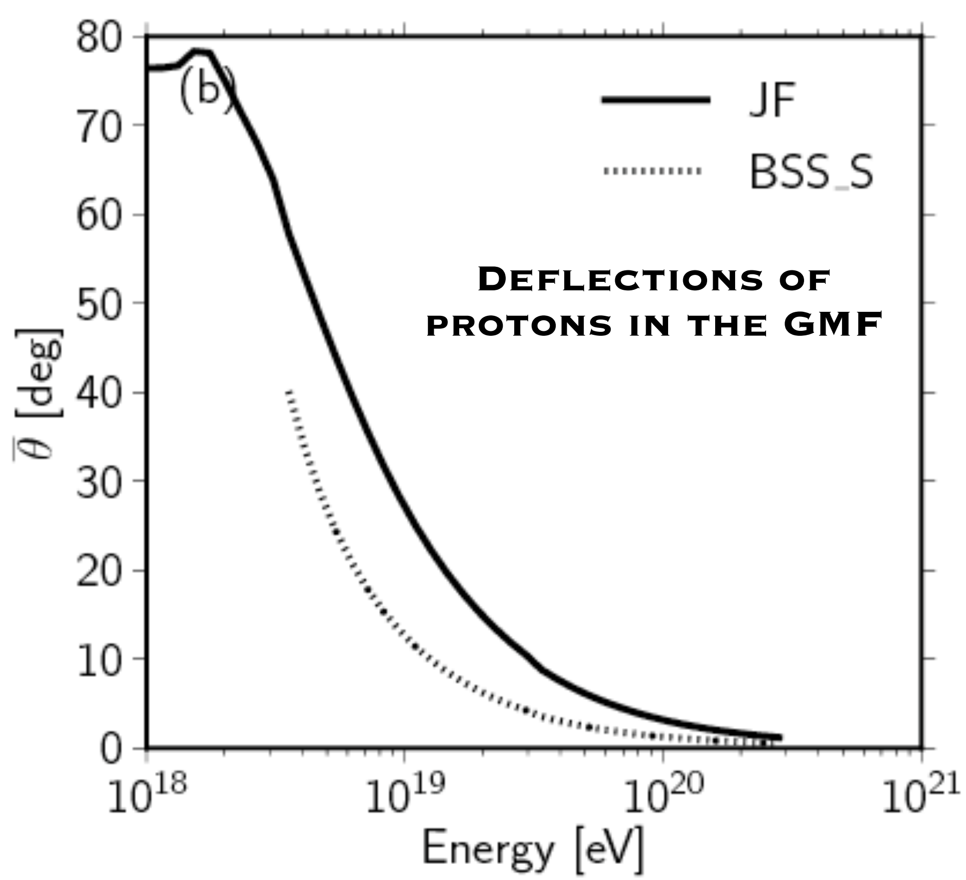

Also, **large-scale anisotropies** can be reflective of either a collective motion of cosmic rays (e.g., of their propagation) or of the global distribution of their sources

UHECR anisotropies: a glance at the past

UHECR detection over the years (up to ≈ 2000)

EITHER giant particle-detectors arrays (100% d.c.)

OR telescopes recording fluorescence light emitted by Nitrogen molecules excited by shower particles (10-15% d.c.)

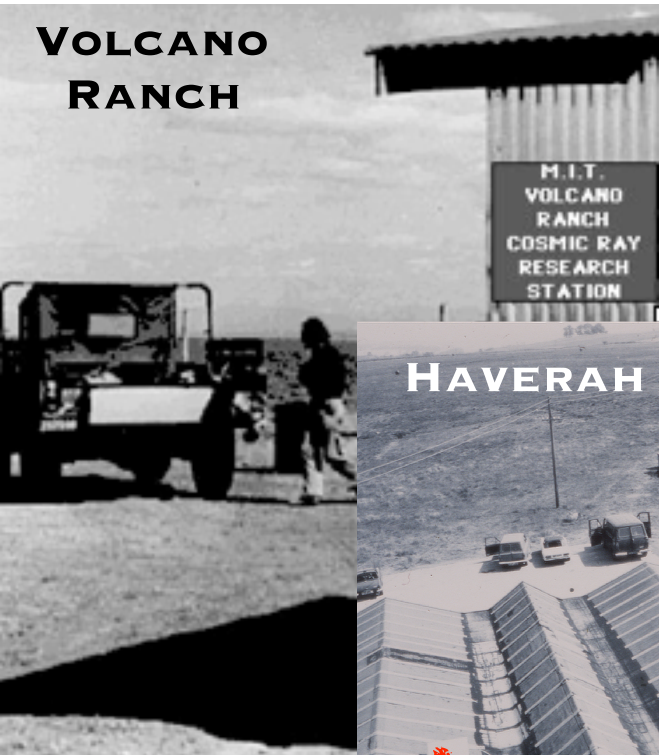

1963 - ≈ 2000

Larger and larger acceptance

7 observatories, ≈ 40 years:

O(1000 km^2 sr y) exposure

UHECR arrival directions, at the beginning of 2000s

Small-scale anisotropies

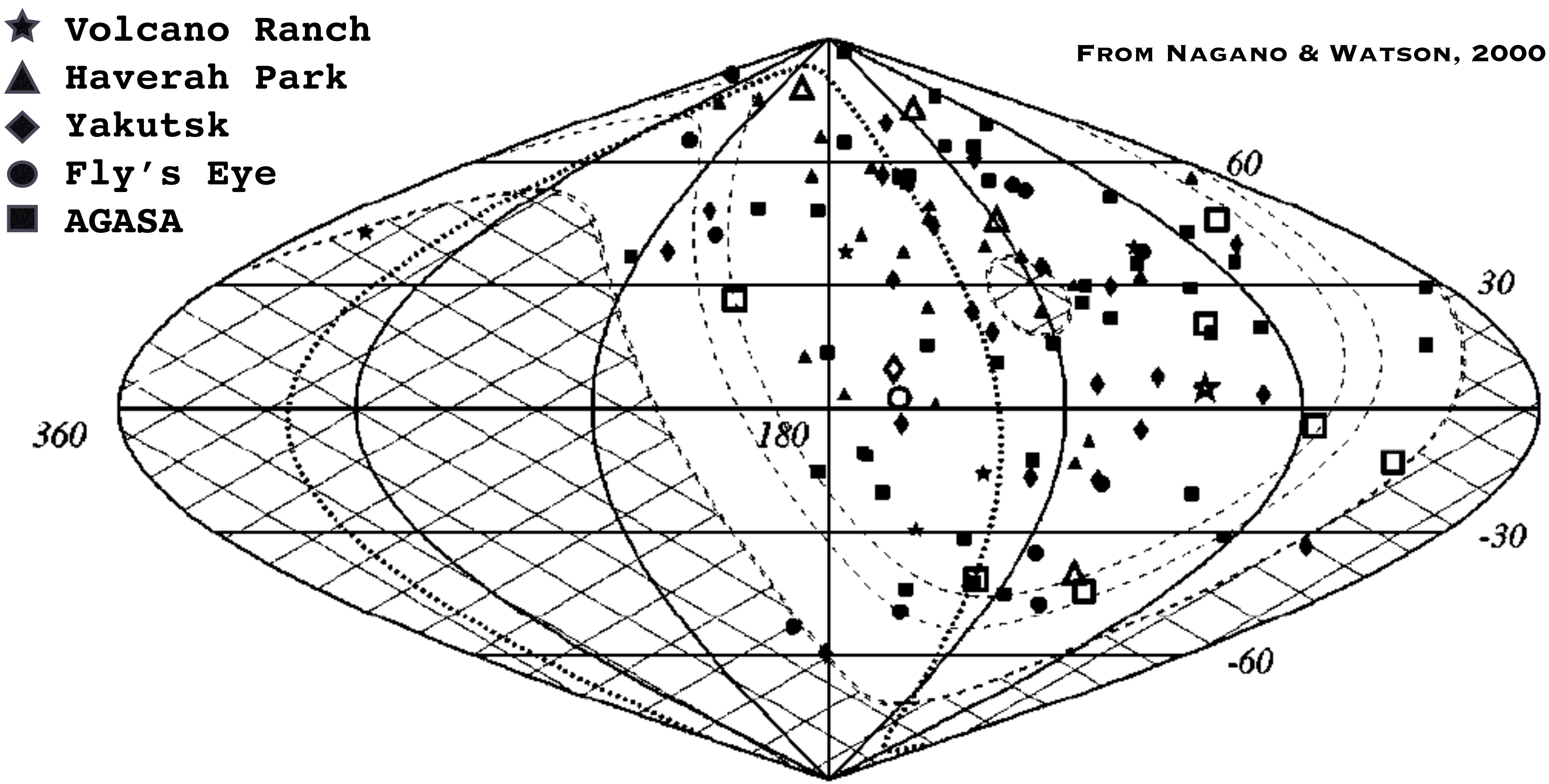

40 years of observation, 5 different experiments:
≈ 100 events above 40 EeV

The scarce number of events was a harbinger of contradictory interpretations in terms of their anisotropy (SG plane? Blazars? Isotropy?)

UHECR arrival directions, at the beginning of 2000s

Large-scale anisotropies:
First harmonic in right ascension

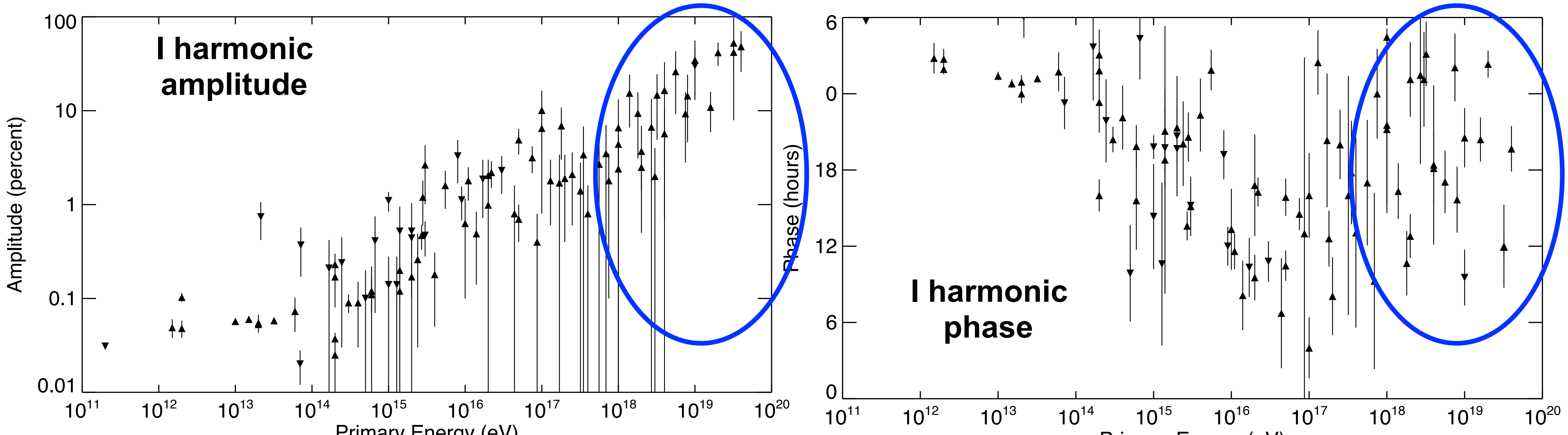

From Clay & Smith, 1997

Scarce number of events:
Low-significance of amplitudes;
“Scattered” phases.
Lack of conclusion on the presence of a large-scale anisotropy at UHE

12

First decade of 2000s: the giants awake

2004:
Pierre Auger Observatory, Malargüe, Argentina
1660 surface detectors (water Cherenkov),
4 fluorescence detectors

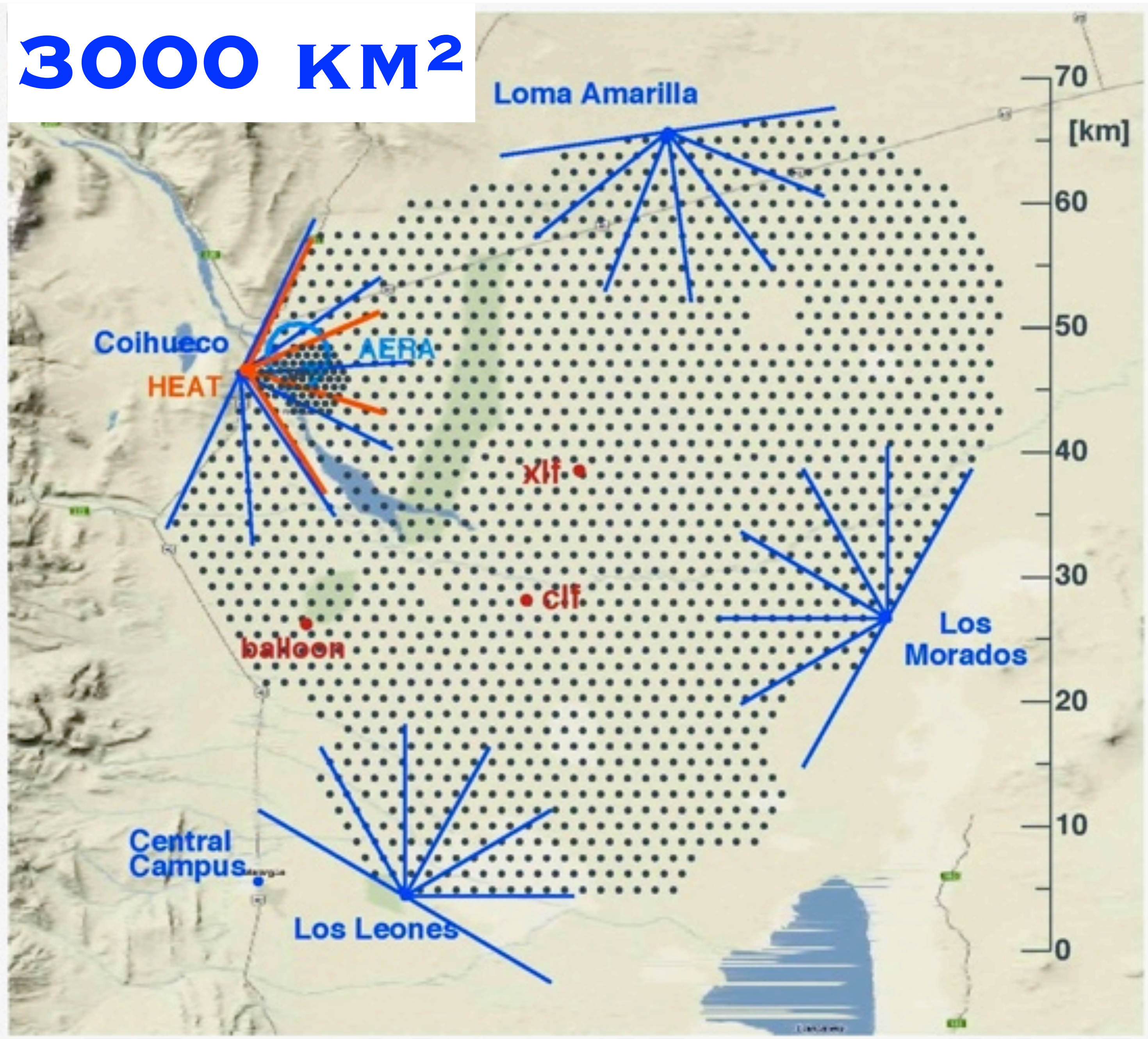

2008:
Telescope Array, Utah, USA
507 surface detectors (scintillators)
3 fluorescence detectors

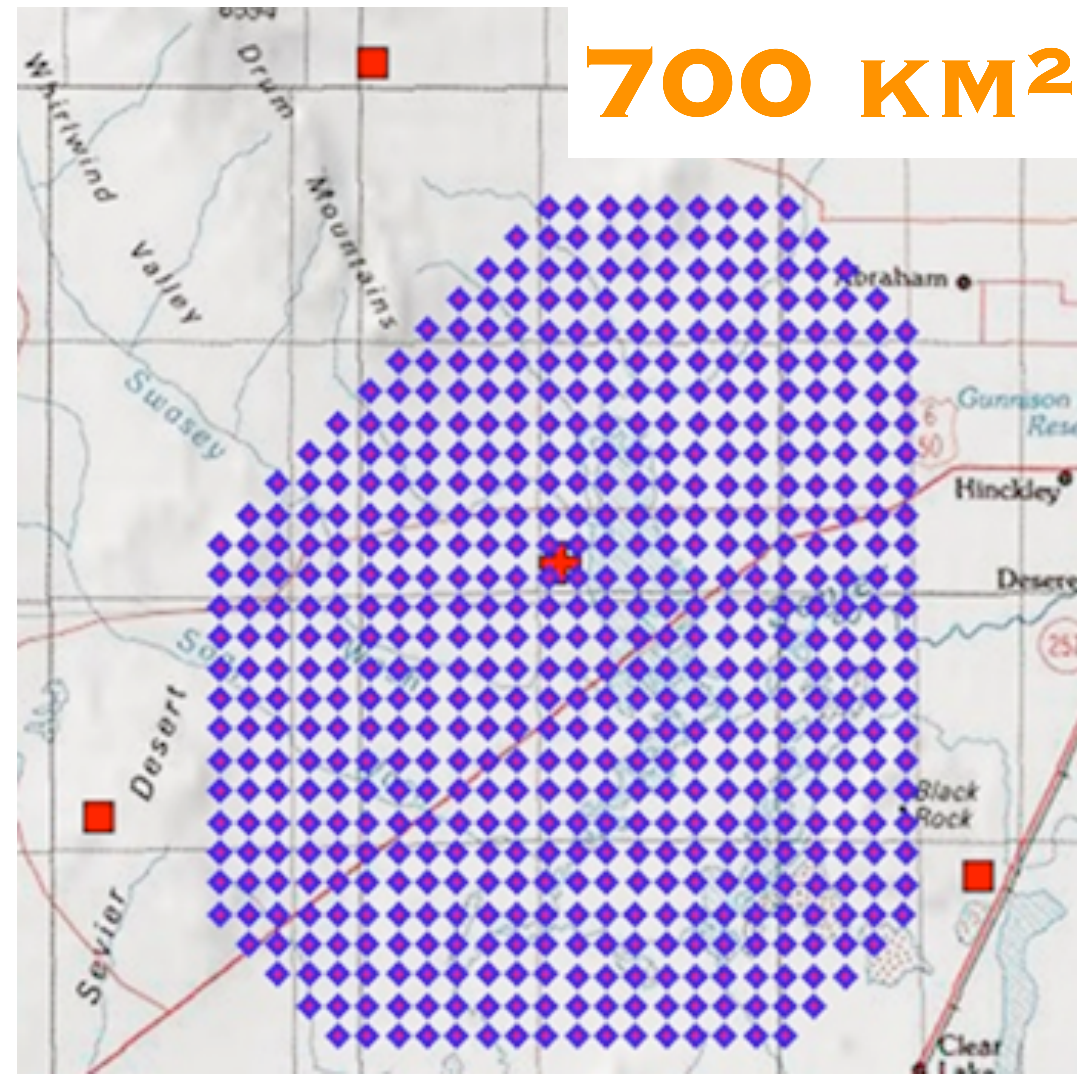

Giant AND smart: particle-detectors array AND fluorescence telescopes:
HYBRID OBSERVATORIES

Smart relative location too

Telescope Array
39.3 N ,112.9 W

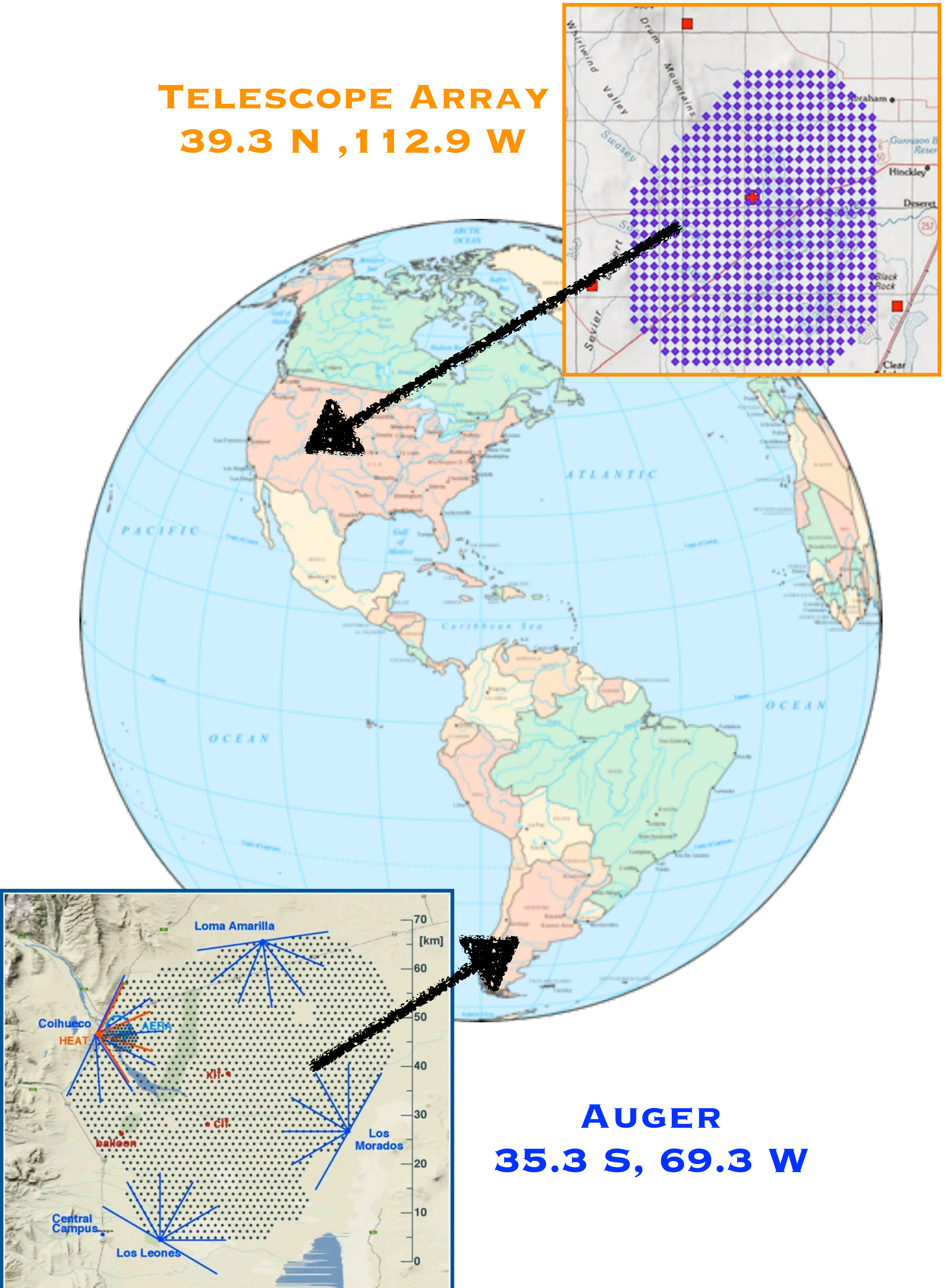

Auger
35.3 S, 69.3 W

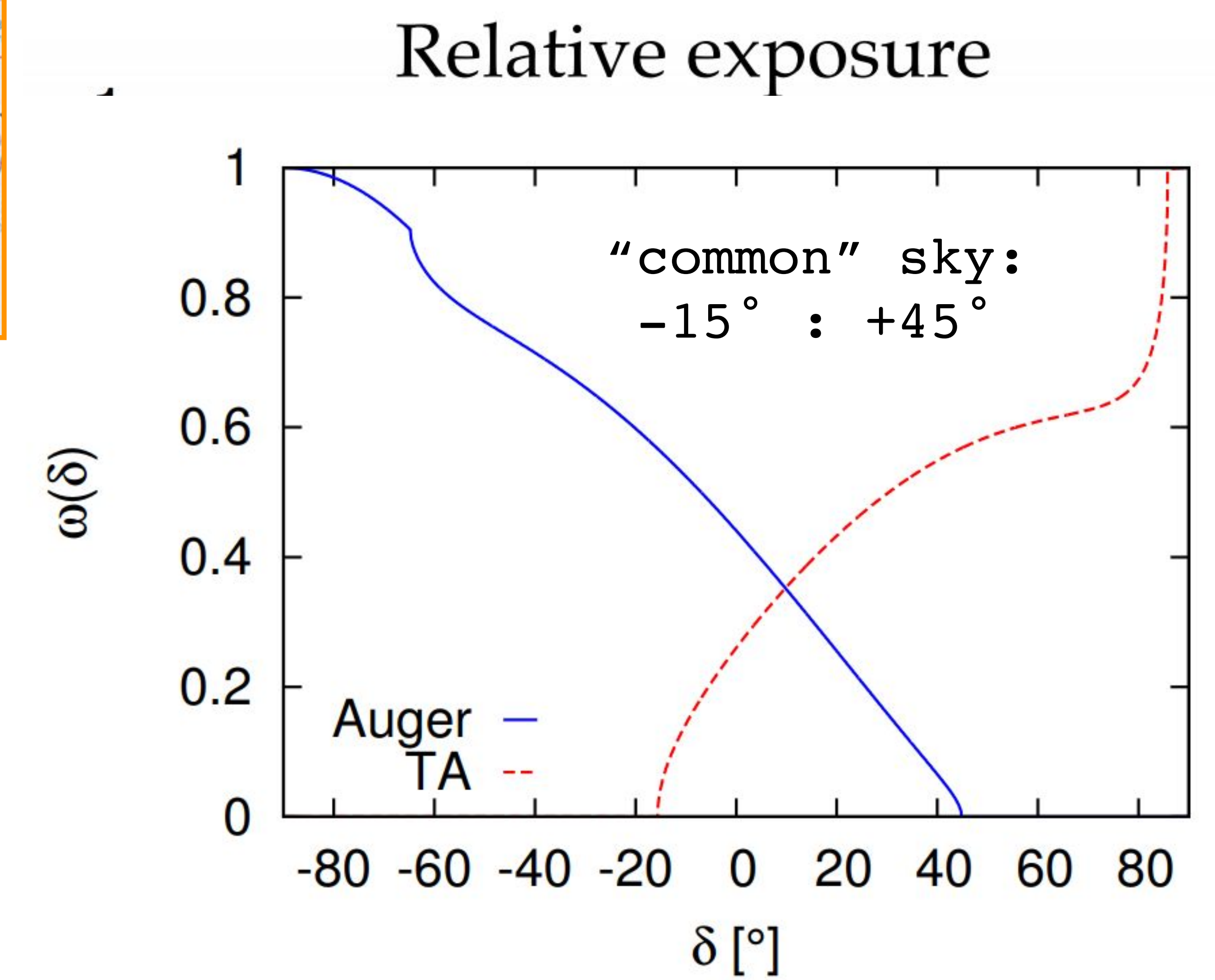

Auger (ϑ: 0-80˚)+ TA (ϑ: 0-55˚)

=

FULL SKY COVERAGE

Auger and TA : directional analyses

Search for anisotropies in the distribution of the arrival directions:
a natural and central quest since the start of their data taking.

Two lines of analyses pursued with increasing statistics:

At "low" energies (O(EeV): "Large" scale studies

- **Aim**: studying the evolution of the amplitude and direction of anisotropy vs energy to identify their origin, galactic vs extra-galactic, and the transition from one to the other. Propagation and/or source distributions may imprint large-scale anisotropy
- **Method**: Harmonic analysis in right ascension (Auger); Spherical harmonic analysis (Auger/TA)

AUGER ALONE
AUGER & TA TOGETHER

At the highest energies ("supra-GZK"): "Small" scale studies

- **Aim**: reducing the "horizon" and exploiting the high rigidity to probe the sources more directly. Only few are capable of accelerating at UHE. Inhomogeneities in their spatial distribution may imprint anisotropy on a smaller scale
- **Method**: Comparison of UHECR arrival directions with astronomical objects (Auger). Search for over densities (TA)

AUGER & TA ALONE
AUGER & TA TOGETHER

Auger and TA: the data

From the surface detector: ≈ 100% duty cycle

Auger

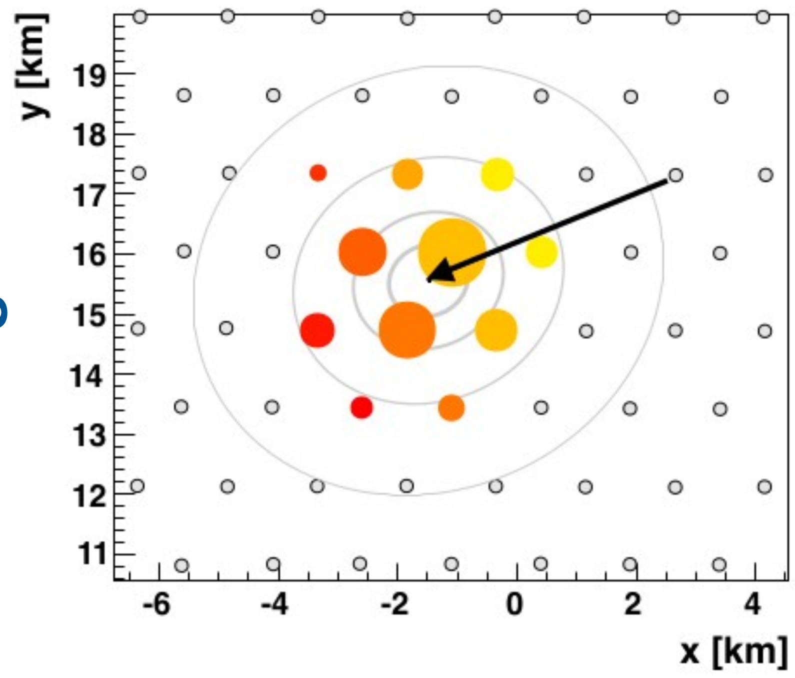

Vertical events, $\vartheta < 60^\circ$

+

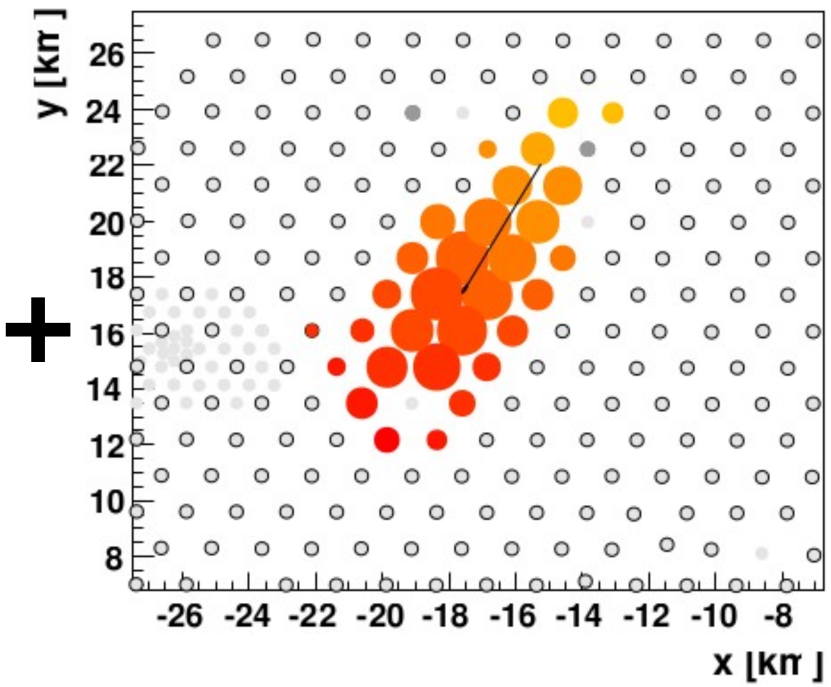

Horizontal events, $60^\circ < \vartheta < 80^\circ$

=

15 y of data
1° unc. arrival direction,
14% syst. unc. energy
E > 4 EeV: full efficiency
(purely geometrical acceptance)

TA

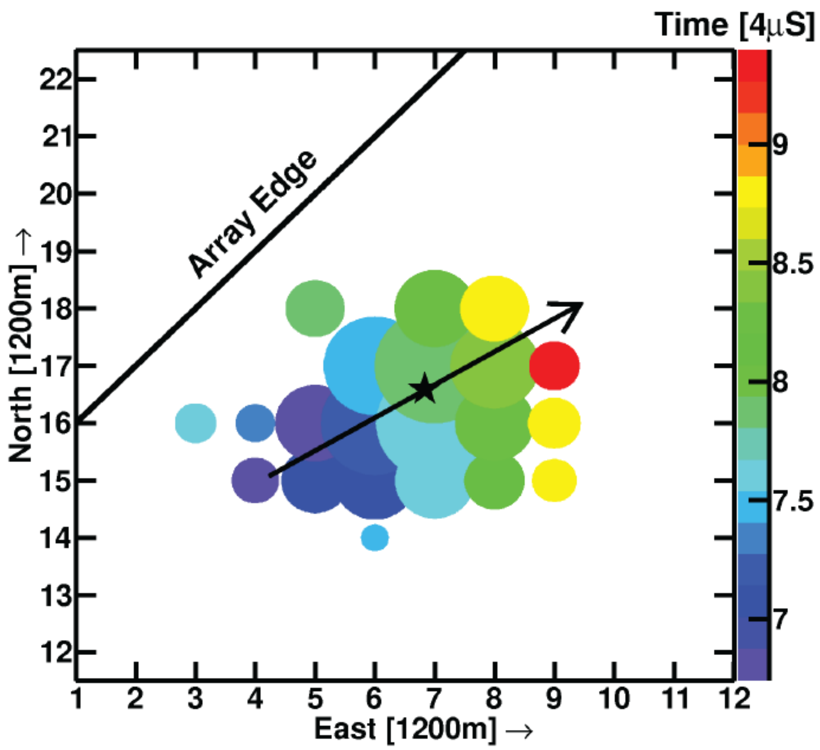

Vertical events, $\vartheta < 55^\circ$

=

10 y of data
1.5° unc. arrival direction
21% syst. unc. energy
E > 10 EeV: full efficiency
(purely geometrical acceptance)

UHECR anisotropies at present: large-scale analysis

Auger large-scale analysis: first harmonic in RA

First harmonic analysis applied in two energy bins (4-8 EeV and > 8 EeV)

[Auger Coll. Science 357 (2017) 1266]

		Harmonic	Components		Amplitude	Phase	Probability
Energy [EeV]	events	k	a_k^α	b_k^α	r_k^α	$\varphi_k^\alpha\,[^\circ]$	$P(\geq r_k^\alpha)$
4 - 8	81,701	1	0.001 ± 0.005	0.005 ± 0.005	0.005	80 ± 60	0.60
≥ 8	32,187	1	-0.008 ± 0.008	0.046 ± 0.008	0.047	100 ± 10	2.6×10^{-8}

4-8 EeV bin:
consistent with isotropy:
r < 0.012 @ 95% c.l.

> 8 EeV bin: r = 0.047 ± 0.008
φ = 100˚±10˚
P(r) = 2.6 x 10⁻⁸ (5.6 s.d.)
Post-trial (two energy bins)*:
5.4 s.d.

E > 8 EeV

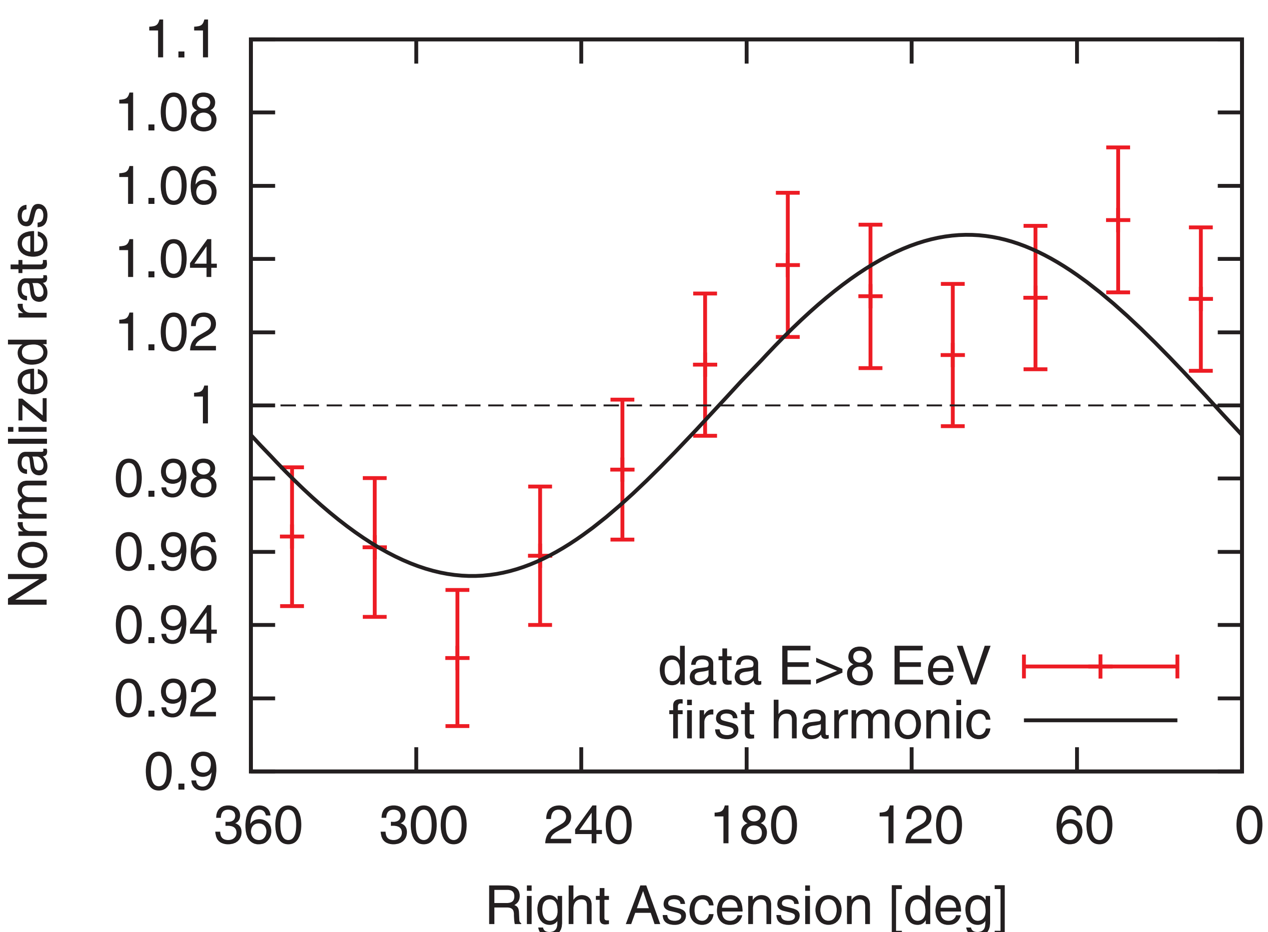

* Post-trial (six energy bins, as in APP, 34, 2011, 627)*: 5.2 s.d.

Auger large-scale analysis: dipole reconstruction

Combination of harmonic analysis in right ascension and in azimuth

[Auger Coll. Science 357 (2017) 1266]

Amplitude: $6.5^{+1.3}_{-0.9}$%

Right ascension: 100˚±10˚, Declination: -24˚±13˚

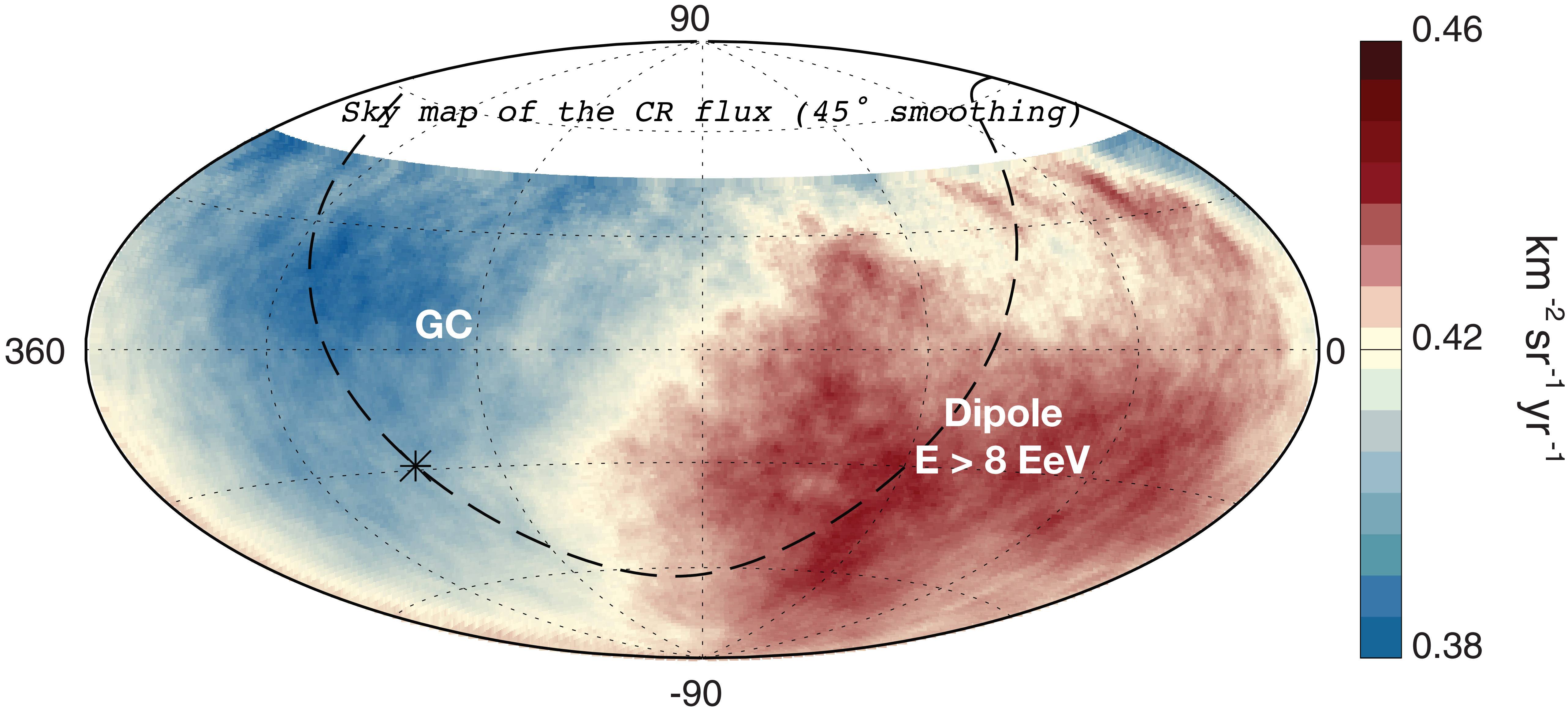

The direction of the dipole lies ≈ 125˚ from the Galactic Center

Direction hard to explain with a Galactic origin

Auger large-scale analysis: UHECRs and "close-by" galaxies

Amplitude: 6.5$^{+1.3}_{-0.9}$%

Galactic longitude: 233˚, Galactic latitude: -13˚

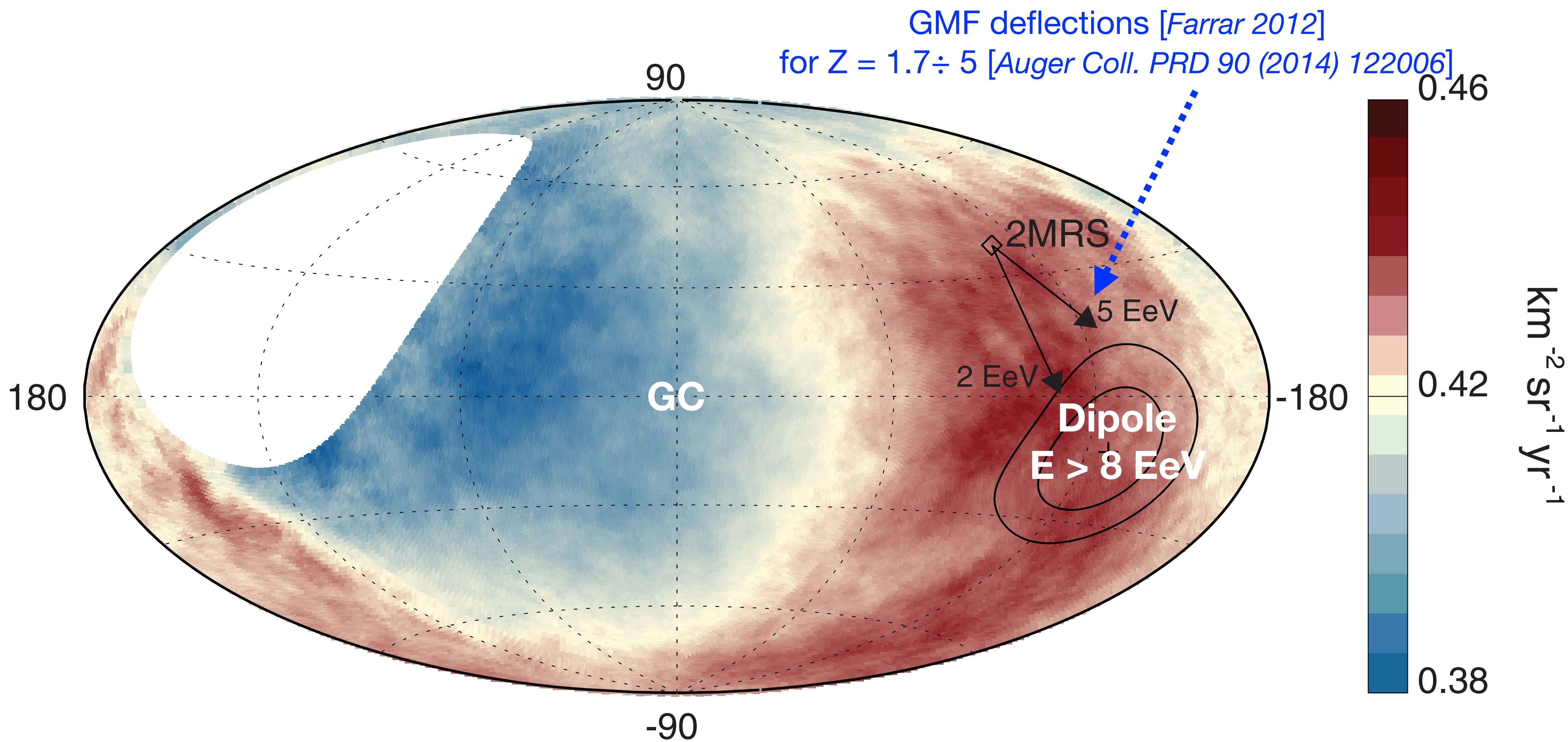

Amplitude: factor 10 > CG effect due to the Earth motion in the CR rest frame.

Larger anisotropies if sources distributed inhomogeneously or CRs diffused by IGMF.

Amplitudes depend on CR composition and source distributions

Appealing rapprochement of the CR dipole direction with that of 2MRS galaxies when CR compositions inferred at these energies are assumed

Auger & TA large-scale joint analysis (work in progress)

Covering the full sky

Sky map of the CR flux (45° smoothing), E > 10 EeV

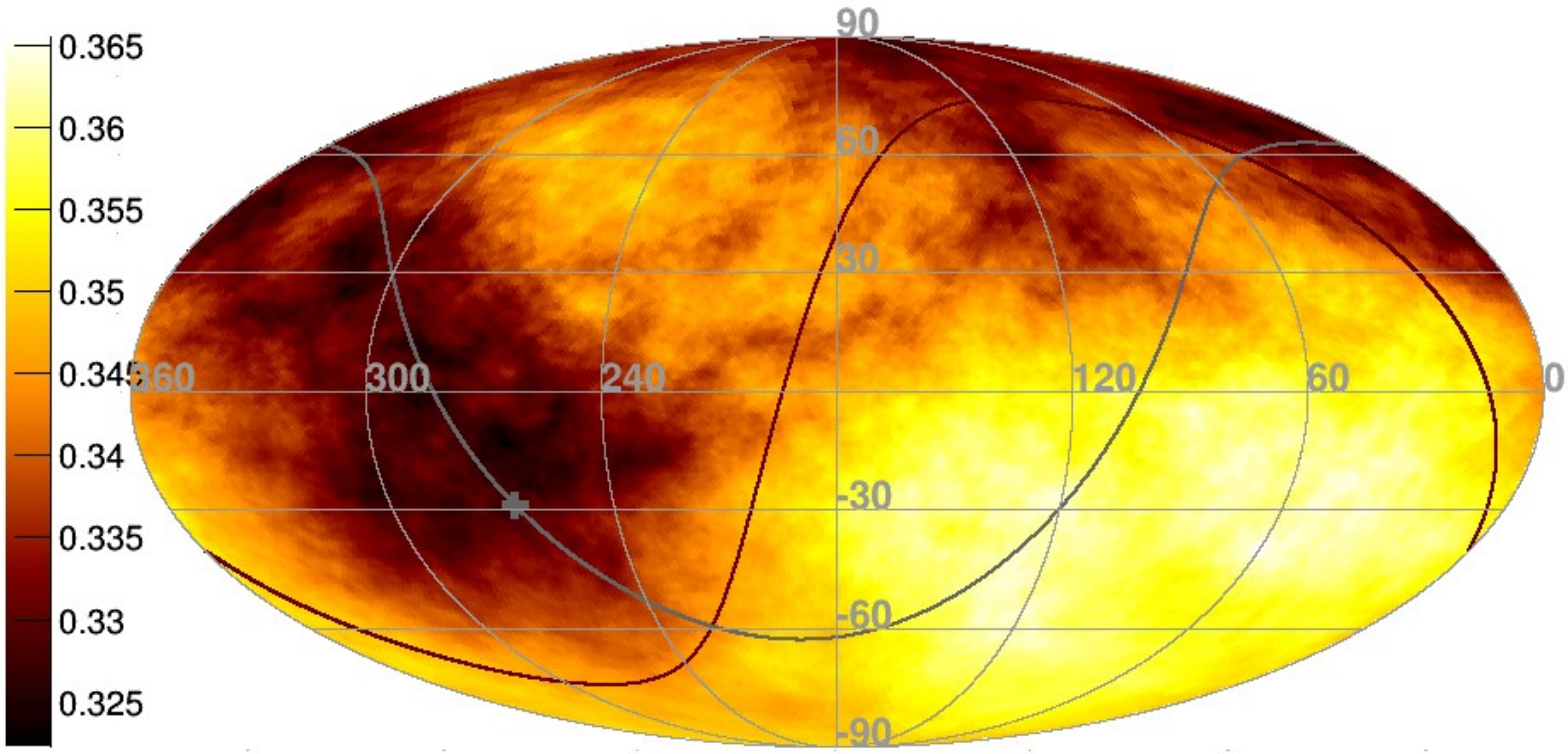

By eye: dipolar pattern similar in shape and amplitude to that observed above 8 EeV
Flux somewhat enhanced in the NW quadrant: possible quadrupole?

Auger & TA large-scale joint analysis (work in progress)

Method: Spherical harmonic analysis
All multipoles accessible with no a priori

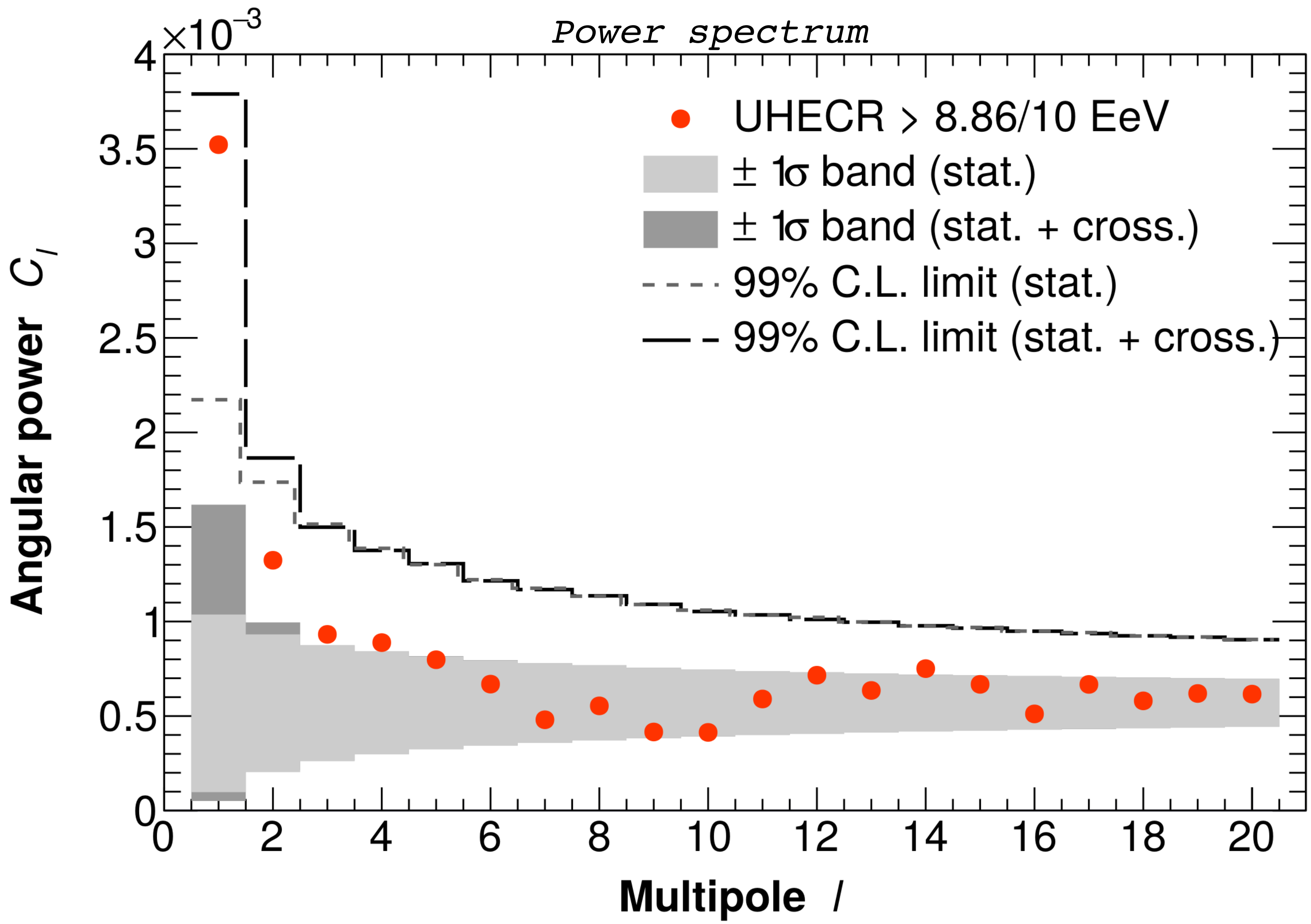

Largest deviation for l = 1 (2.5. s.d.)

Small deviation also for l = 2 (1.9 s.d.): quadrupole to be further studied

UHECR anisotropies at present: “small”-scale analysis

Auger "small"-scale analysis:"close-by" galaxies

The candidate galaxies and the analysis method

[Auger Coll. ApJL 853 (2018) L29]

γ-ray AGNs from the 2FHL catalog

(Fermi-LAT, E>50 GeV)

R < 250 Mpc

17 objects (among which Cen A, M87, Mkn 421, Mkn501…)

γ-ray flux used as proxy for the UHECR flux

γ-ray SBGs searched by Fermi-LAT

(from the HCN survey)

R < 250 Mpc

Radio-flux > 0.3 Jy

23 objects (among which M82, NGC253, and other 5 detected in γ)

Radio-flux used as proxy for the UHECR flux

Method: Unbinned maximum LH analysis

UHECR sky model: isotropy + anisotropic component from the sources

Directional exposure accounted

TS = LH ratio between H(UHECR sky model) and H(isotropy)

TS maximised vs search radius, ϑ, and anisotropic fraction, α

Test repeated over several energy thresholds (E > 20 EeV, up to E > 80 EeV, 1 EeV steps)

Flux attenuation accounted for at each energy threshold

Composition inferred by Auger data accounted for

Auger "small"-scale analysis: results

≈ 5500 UHECRs exploited (≈ 90000 km² sr y)

[Auger Coll. ApJL 853 (2018) L29]

AGNs

TS is maximum for E > 60 EeV (177 events)

SBGs

TS is maximum for E > 39 EeV (894 events)

TS as a function of energy threshold

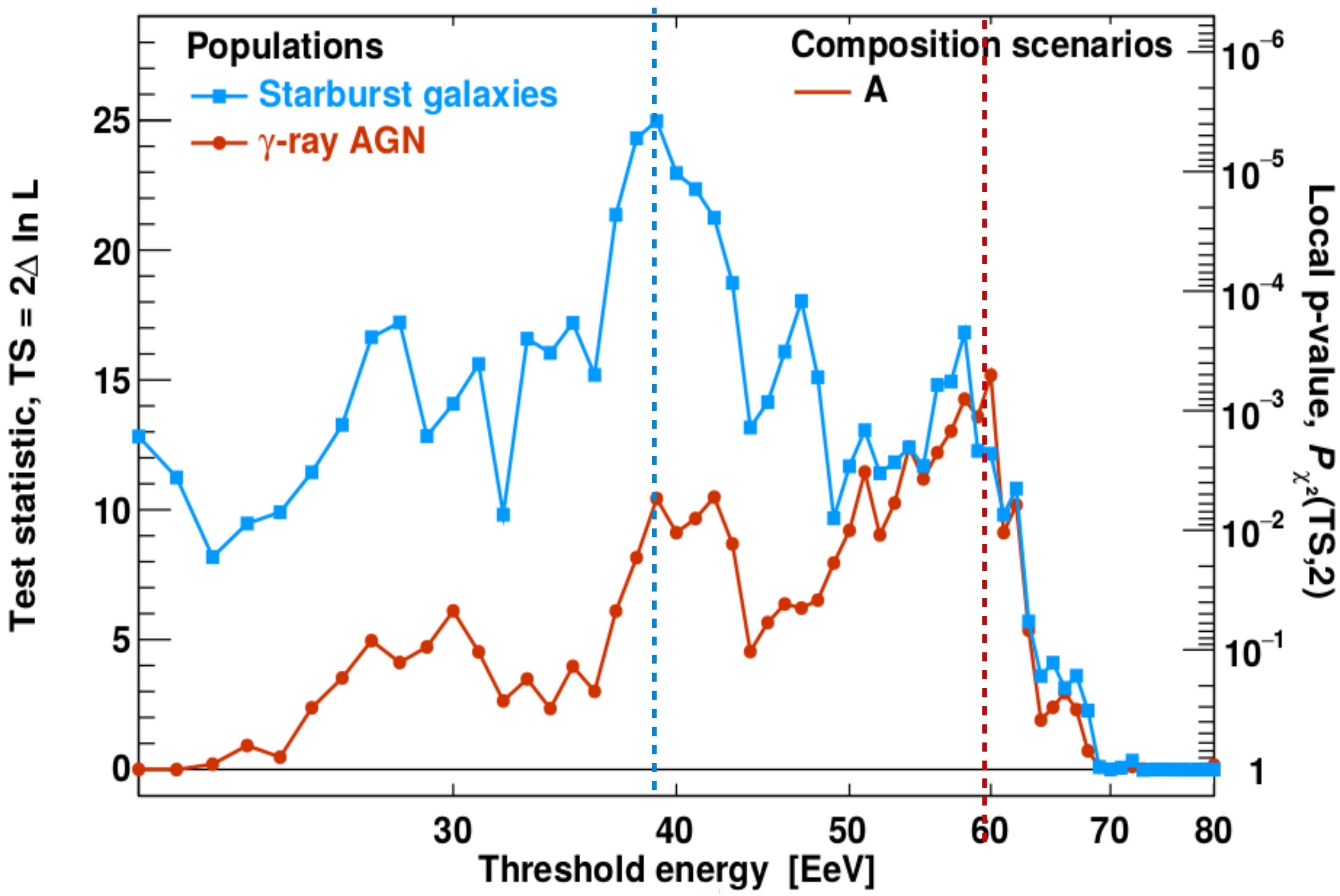

Auger "small"-scale analysis: results

≈ 5500 UHECRs exploited (≈ 90000 km² sr y)

[Auger Coll. ApJL 853 (2018) L29]

AGNs

TS is maximum for E > 60 EeV (177 events)

α = 7 ± 4%, ϑ = 7° ± 4°

Post-trial (2 par. and E scan): 2.7 s.d.

SBGs

TS is maximum for E > 39 EeV (894 events)

α = 10 ± 4%, ϑ = 13° ± 4°

Post-trial (2 par. and E scan): 4.0 s.d.

Maximum TS: radius and anisotropy fraction

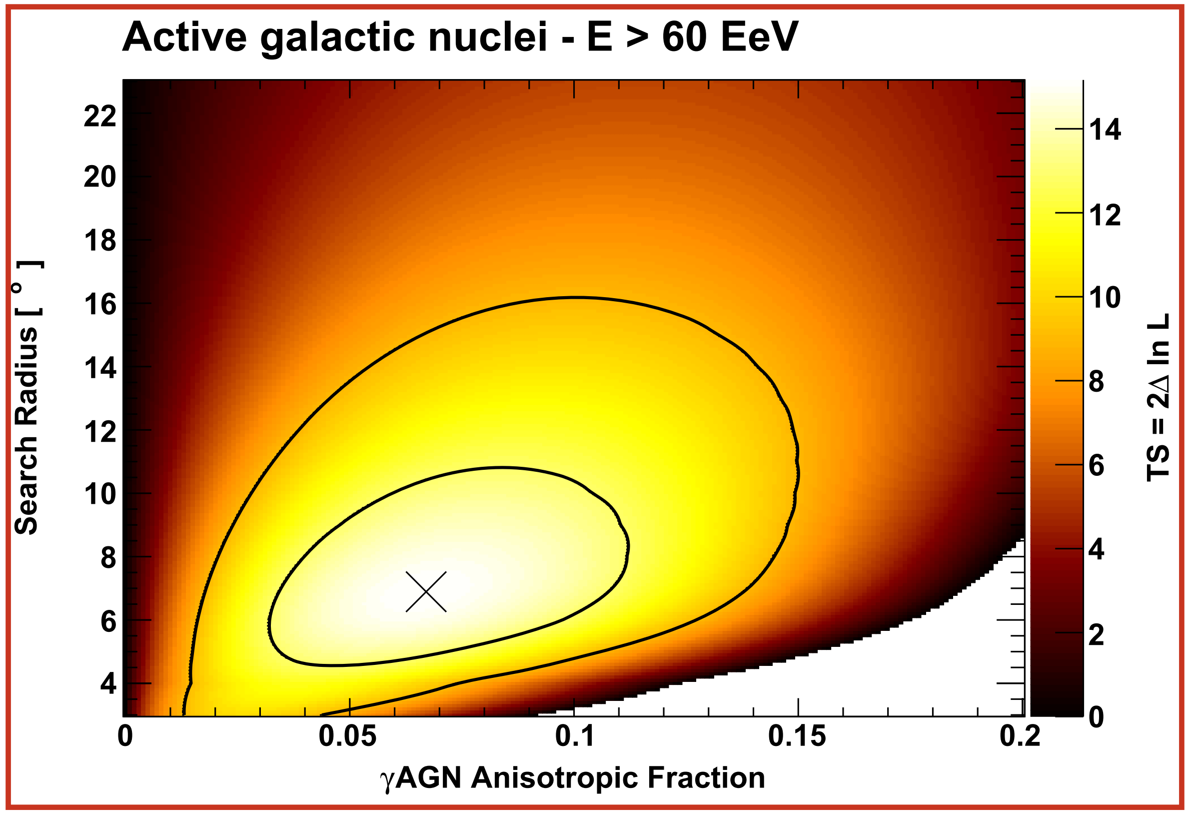

Maximum TS: radius and anisotropy fraction

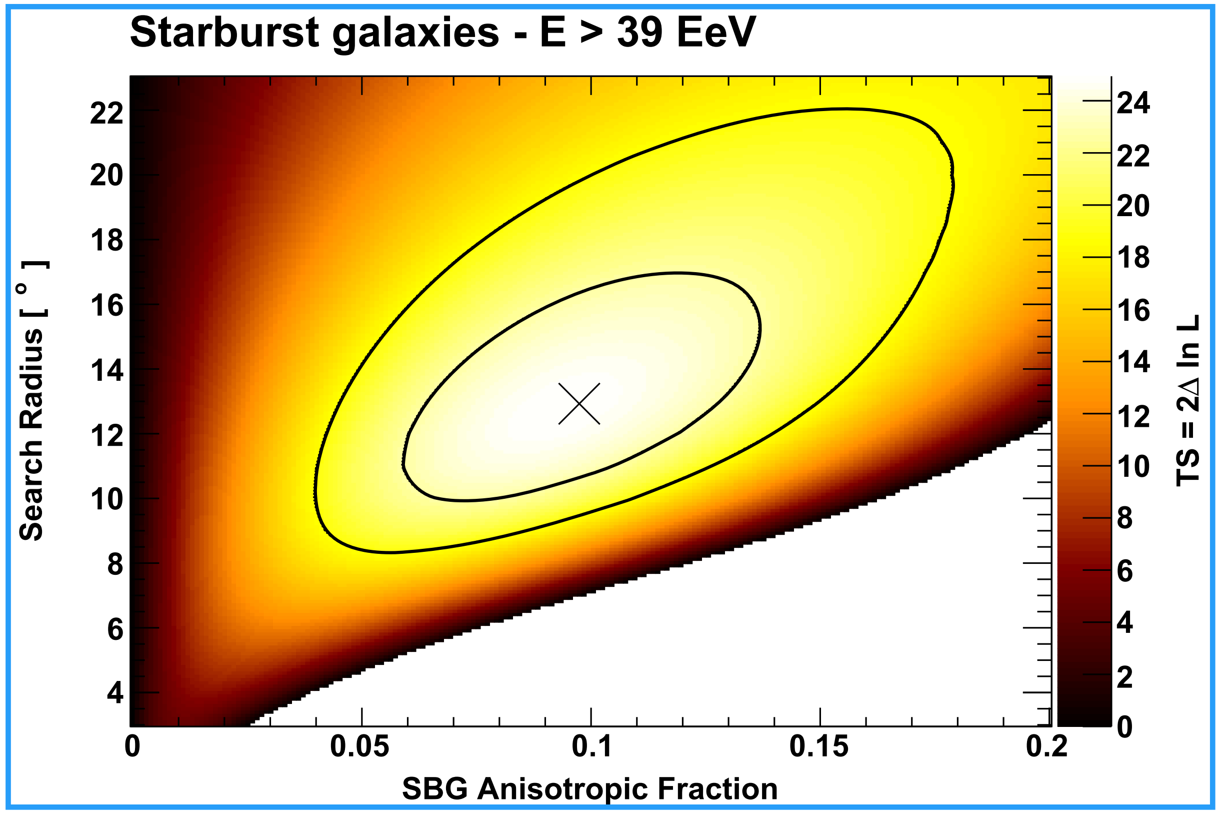

Comparison with SBGs indicates that isotropy is disfavoured with 4 s.d. significance (post-trial)

TA "small"-scale analysis: search for over-densities

Angular Scan
(>57EeV,10 years)

Preliminary

O.S. : oversampling radius

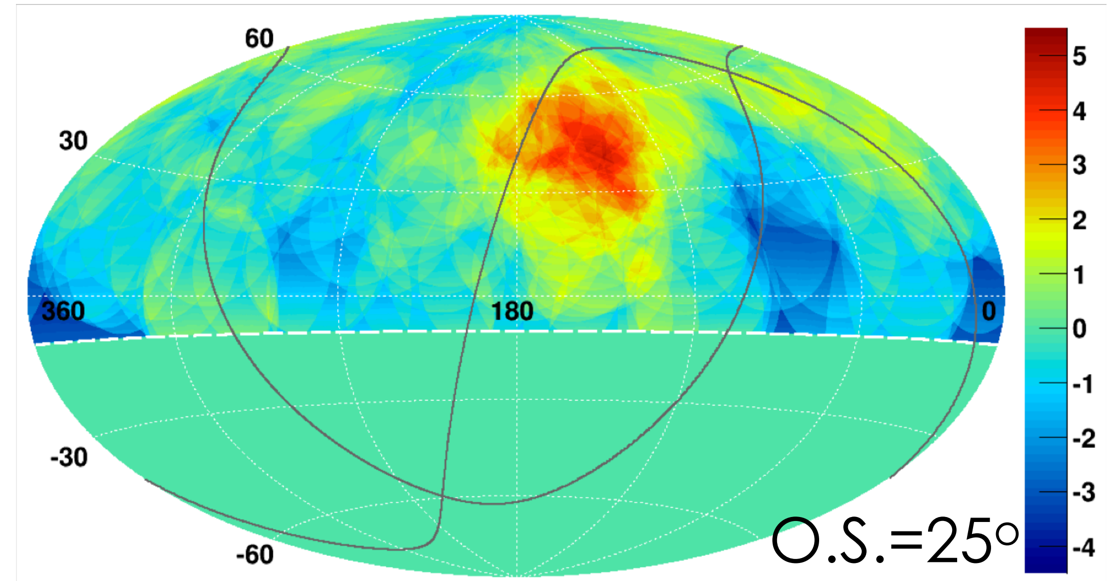

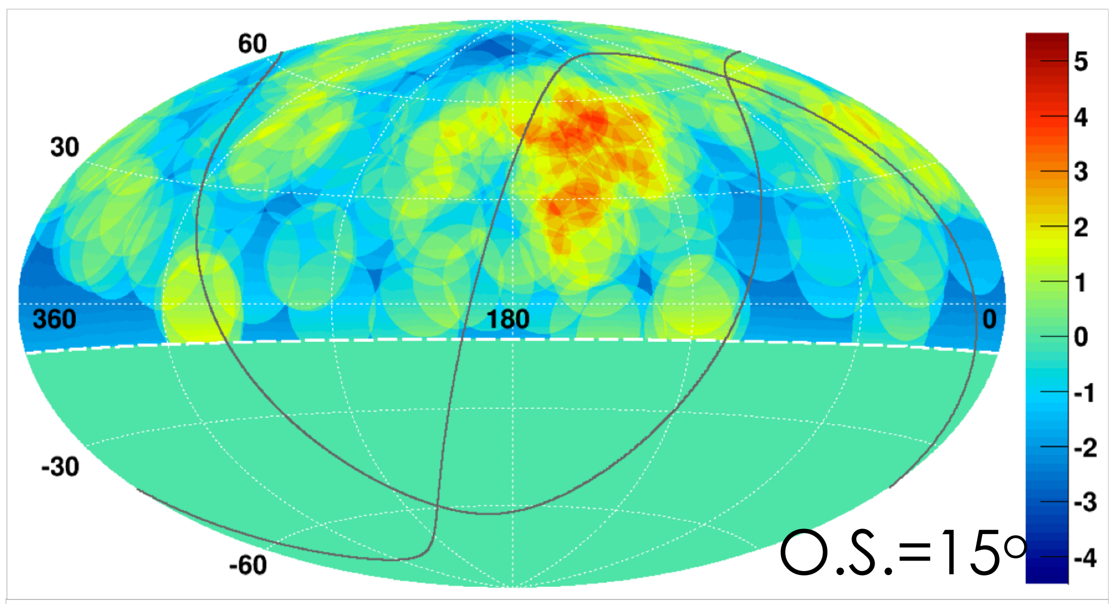

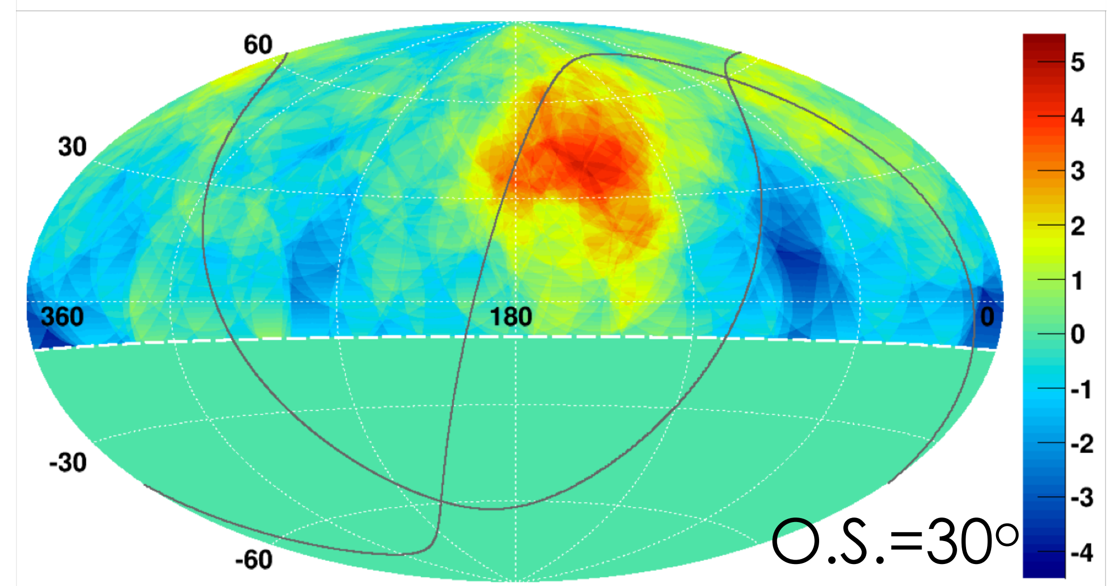

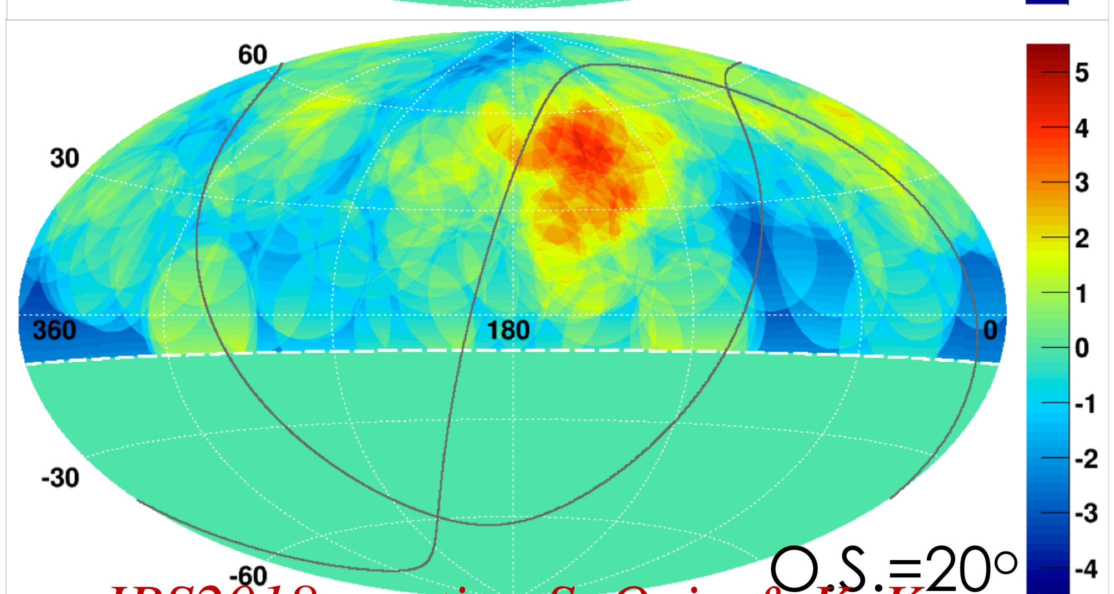

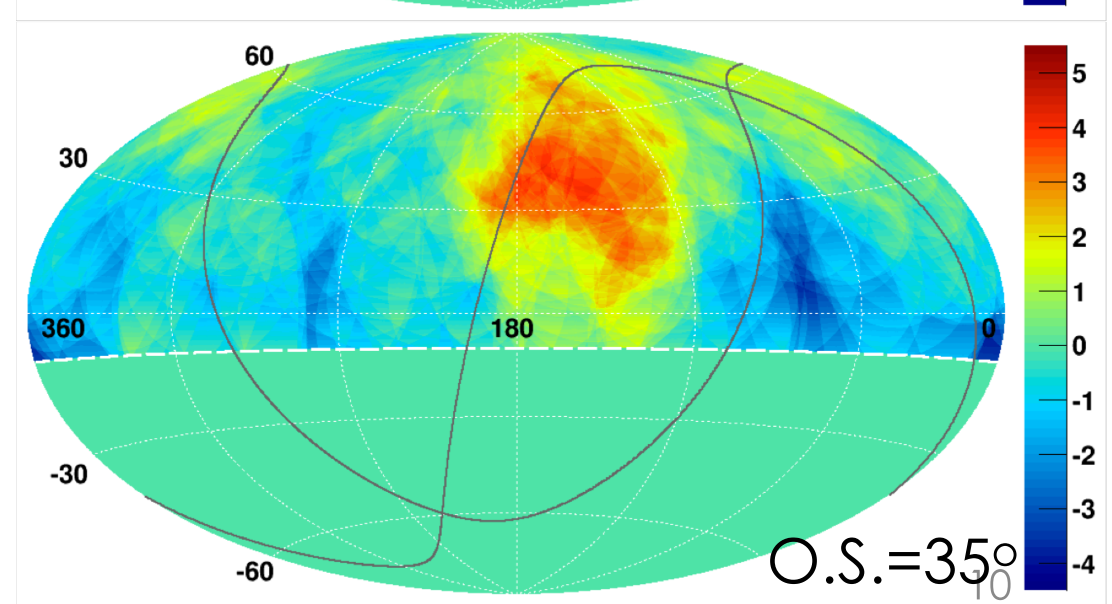

From JPS2018 meeting S. Ogio & K. Kawata

TA “small”-scale analysis: search for over-densities

Results of the Angular Scanning for 10 years

Preliminary!

O.S. radius	15°	20°	25°	30°	35°
Maximum Significance for 10 years (σ)	4.1	4.6	5.0	4.7	4.2
Location of Maximum Significance	RA:140.4° Dec: 53.2°	RA:149.4° Dec: 49.0°	RA:144.3° Dec: 40.3°	RA:152.8° Dec: 39.8°	RA:157.4° Dec: 38.5°

Hotspot position published in ApJL2014 → RA: 146.7° Dec: 43.2°

From JPS2018 meeting S. Ogio & K. Kawata

Auger and TA: “small”-scale analysis

Most significant excesses at intermediate angular scales

Auger

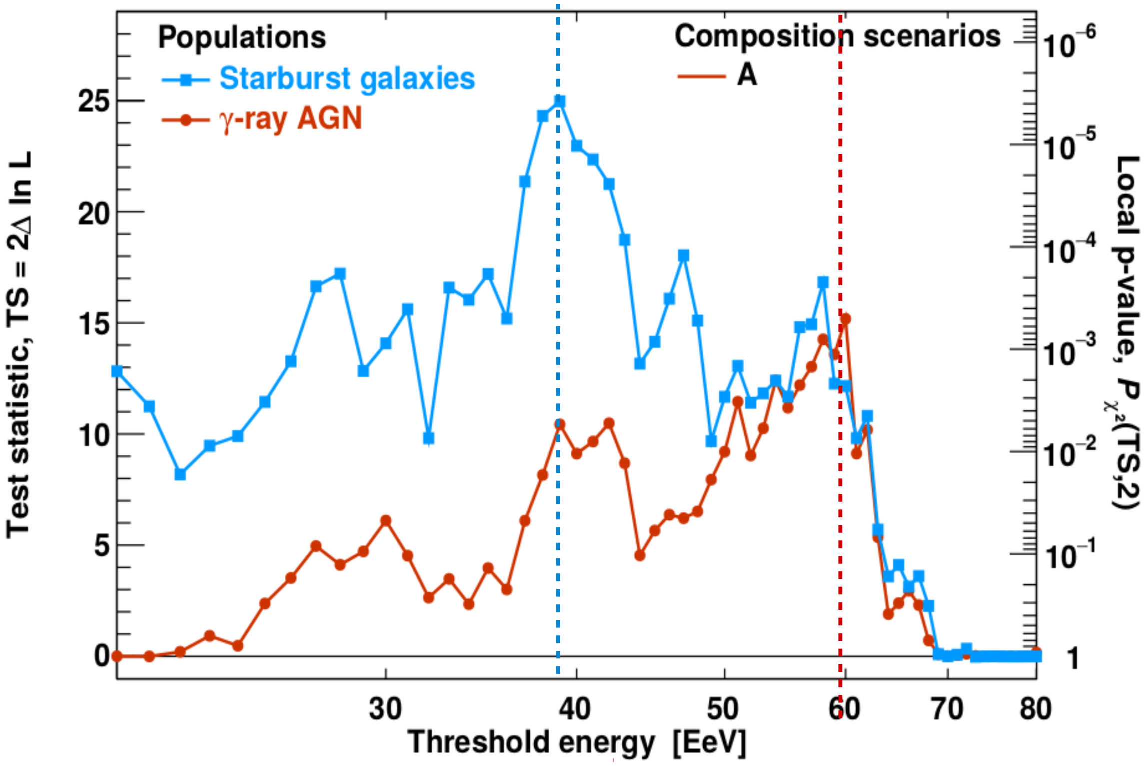

Starburst Galaxies (d<250 Mpc)
Smallest p-value at 39 EeV, r=13˚
Post-trial: 4 s.d.

TA

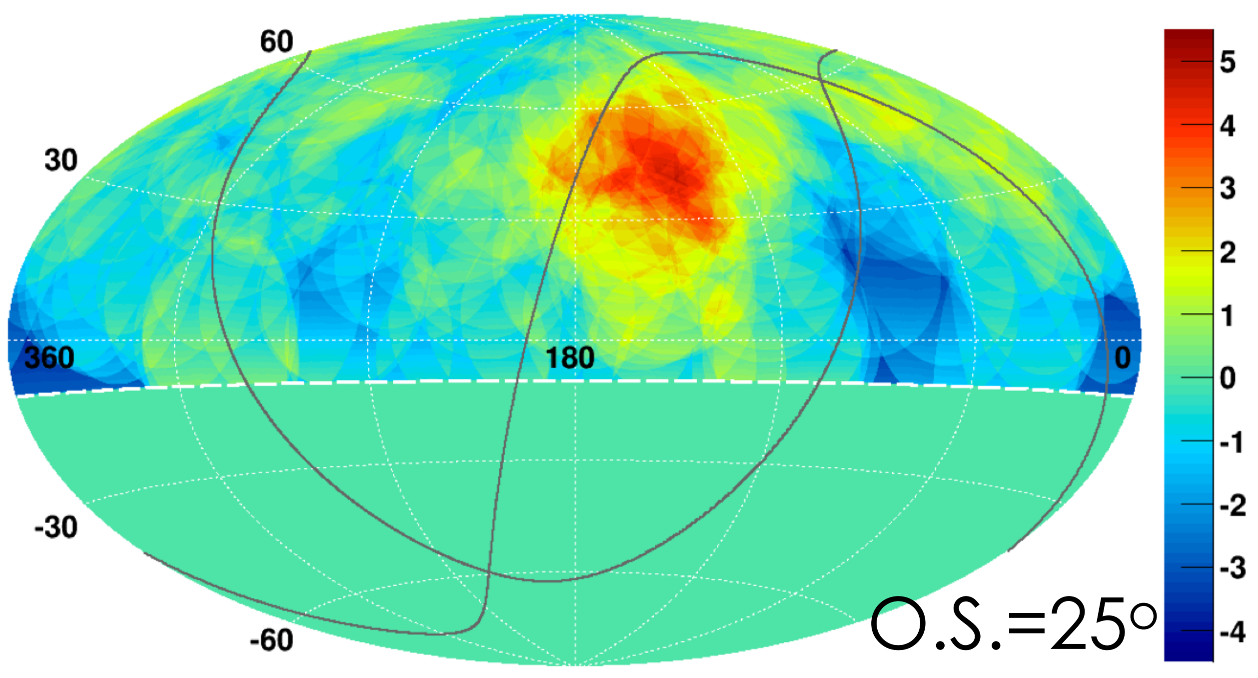

Hot spot (10 yr)
E>57 EeV, r=25˚
Post-trial: 3 s.d.

No evidence of small-scale anisotropy,
but indication of intermediate-scale anisotropy
N.B. The very luminous SBG M82 is partly overlapping with the TA hotspot.

Auger and TA: "small"-scale joint analysis

Full sky

Flux map

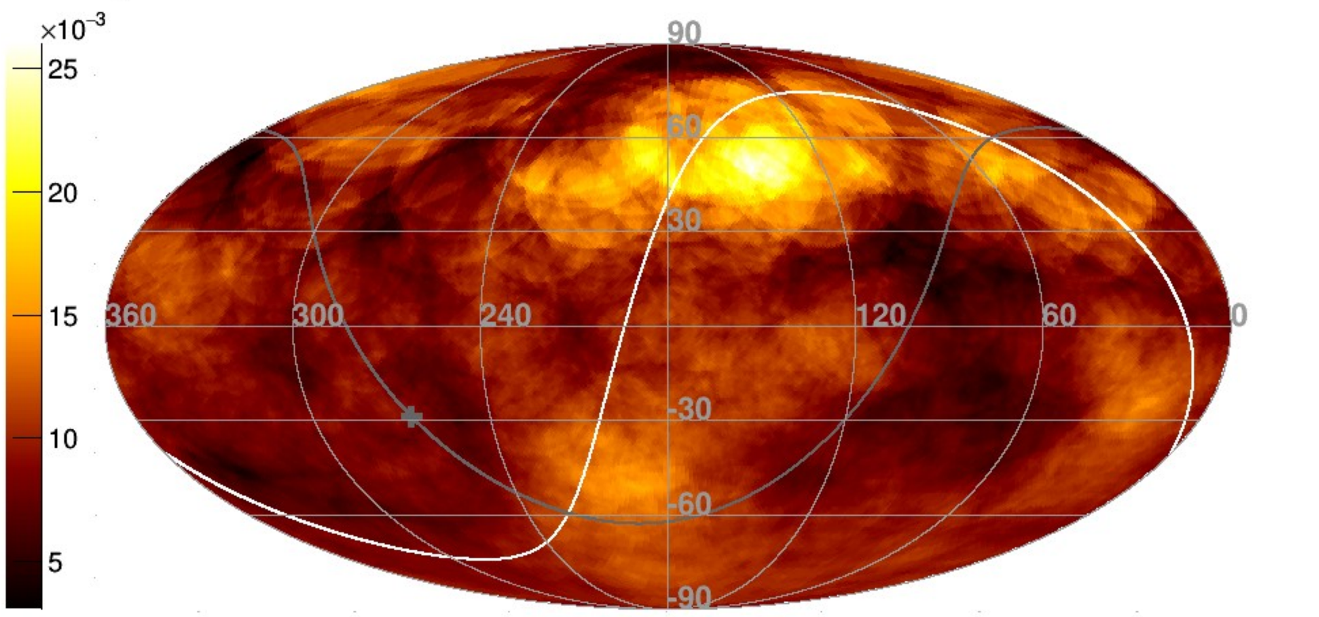

Significance map

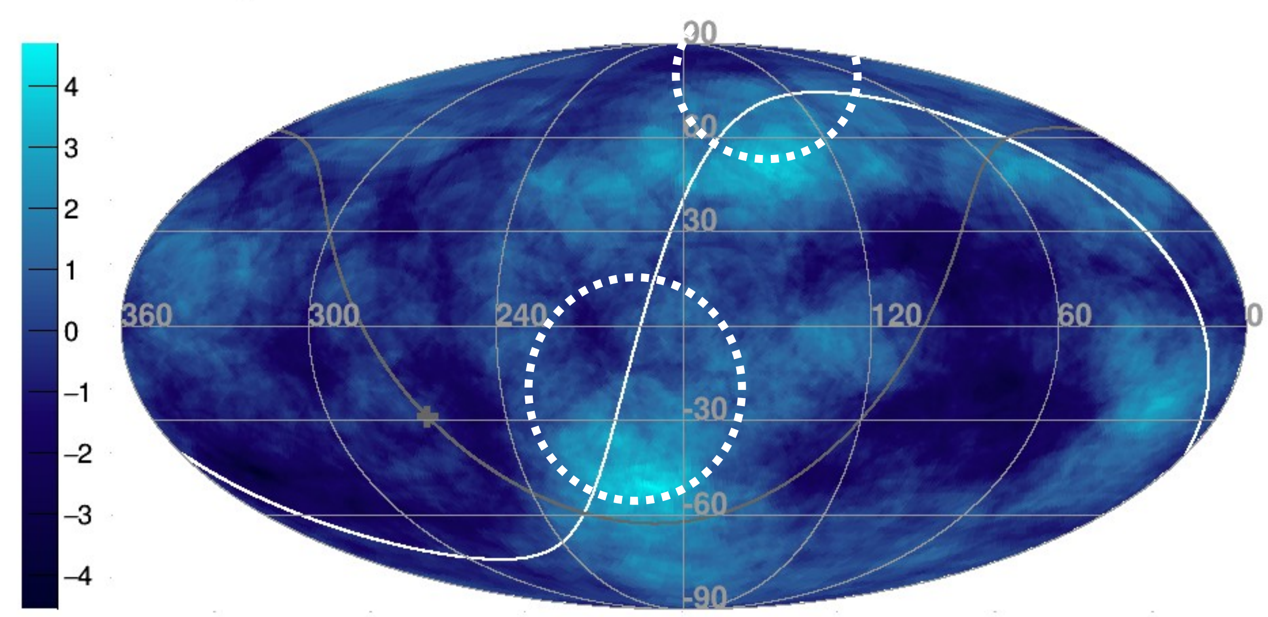

Spherical harmonic analysis of flux map

Power spectrum: largest deviation for C_{14} (2.8 s.d.) corresponding to an angular scale 180/14 ≈ 13° (Post-trial: 1.6 s.d.)

No indication of deviation from isotropy from full-sky power spectrum

Two warm-spots along the SG plane

Largest significance: 4.7 s.d. @ 20°

II largest significance: 4.2 s.d. @ 15°

Post-trial: 2.2/1.3 s.d.

Conclusions (so far)

"Large" scale studies

- **Discovery (> 5 s.d.) at E > 8 EeV** of a 4.7% anisotropy in α, with φ=100˚±10˚
- **Assuming a purely dipolar* anisotropy,** its amplitude is d = $6.5^{+1.3}_{-0.9}$% pointing at (α,δ)=(100˚, -24˚)
- The **direction** (> 100˚ from the GC) supports the hypothesis that CRs at these energies are **extragalactic**
- The **amplitude** is much larger than expected from a motion-origin (CG), hinting at a **"source-origin"**

"Small" scale studies

- **Indication (4 s.d.) at 39 EeV** of an anisotropy at intermediate scales (≈ 13˚) in association with **Starburst Galaxies**
- **Smaller indication** when studying other source catalogs (AGNs, 2MRS, Swift-BAT) tested
- **Indication (3 s.d.)** at 57 EeV of a hotspot in the northern emisphere at intermediate scales (25˚)
- Warm spots along the SG plane?

* Assuming a dipole+quadrupole, none of the quadrupole components is statistically significant [arXiv 1808.03579]

A look at the future…

- **“Small” scales: increase statistics at UHE (Auger, TAx4).** Confirm the SBGs-based anisotropy? Hotspot?
- **Large scales: go to lower energies,** to probe the Galactic-to-extragalactic transition.
- **Large and “small” scales: keep pursuing full sky analyses Auger & TA.** Higher order multipoles? Correlation with the SG plane? Relate large to intermediate angular scales?
- **Large and “small” scales: mass-discrimination criteria** in anisotropy analyses. **AugerPrime**

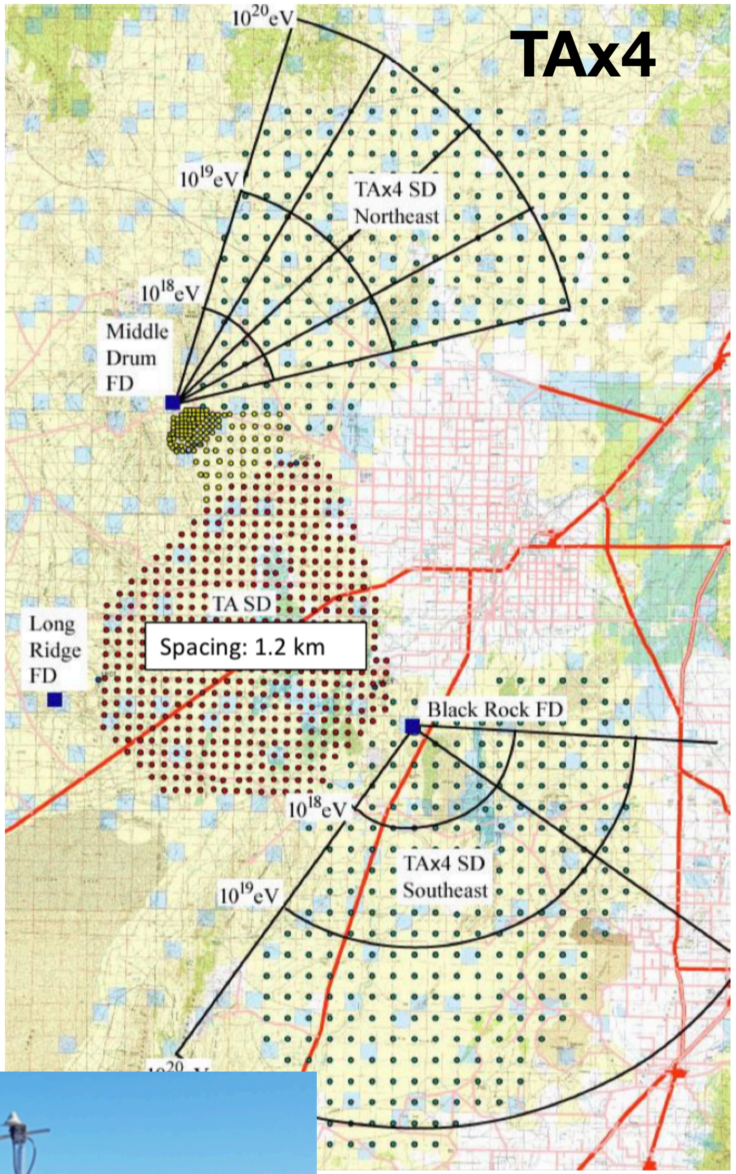

Backup

The smartness of the hybrid technique

Hybrid events allow for the calibration of the SD energy estimator with the FD calorimetric energy

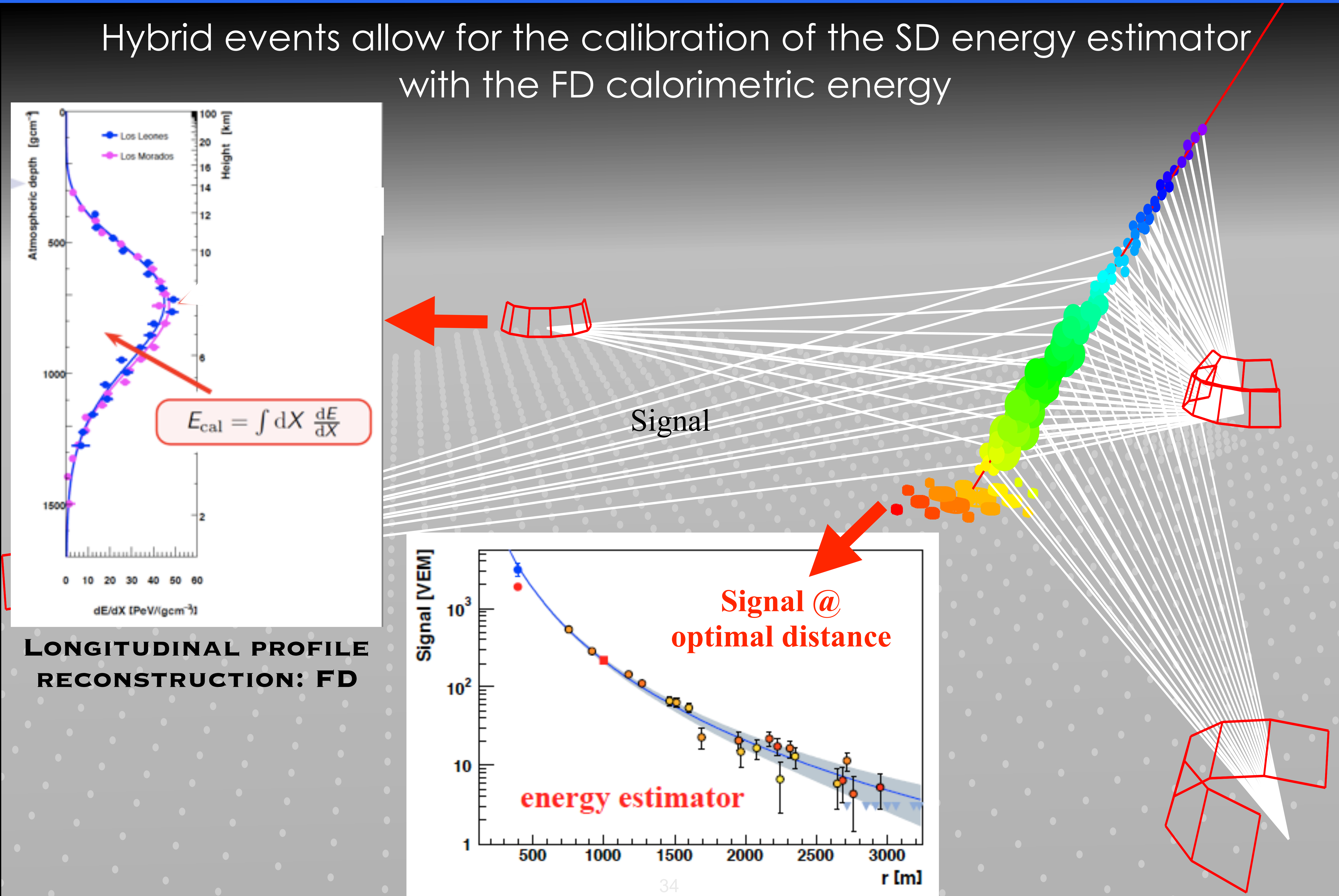

Longitudinal profile reconstruction: FD

Particle lateral distribution: SD

The data: systematic effects

Correction for atmospheric and geomagnetic effects

[Auger Coll. JINST 12 P02006 (2017), JCAP 11 (2011) 022]

Atmospheric effects:
Impact on the absorption of em component due to P and T variations.
Energy correction on vertical events.
No correction on horizontal ones (mostly muons).

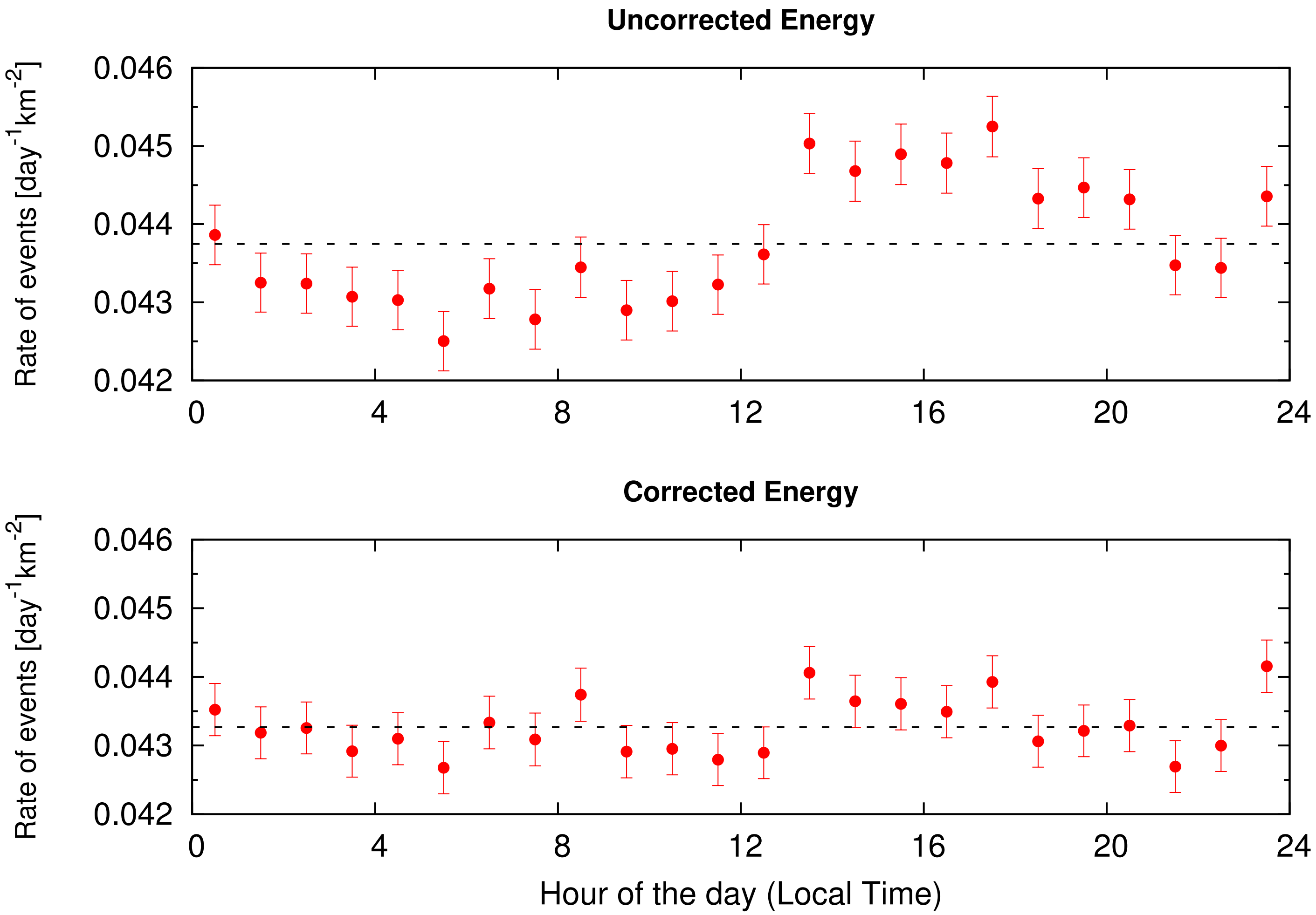

Uncorrected:
± 1.7% variations in solar time

Corrected:
Amplitude 0.5 ± 0.4%

Geomagnetic effects:

Impact on the circular symmetry of the shower. Larger effect at larger angles.
If uncorrected, it would induce modulation in azimuthal angle (0.7%).
Energy correction on both vertical and horizontal events.

The exposure: systematic effects

Purely geometrical exposure controlled at second level

[Auger Coll. NIM A613 (2010) 29]

Geometrical exposure:

Fiducial cuts to ensure containment.
Events used only above the energy yielding full efficiency (E > 4 EeV)
Exposure = sum of active "elementary cells"/sec integrated over time

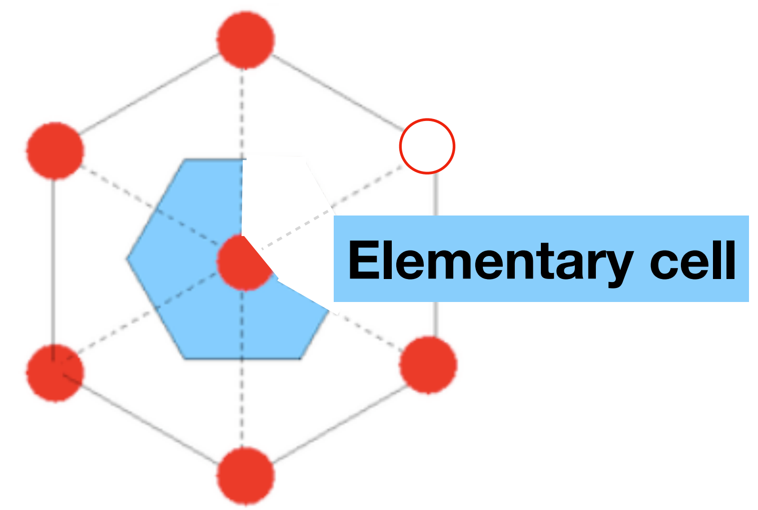

Control of the exposure:

The number of "cells" is not constant (maintenance, power, communications…)
Amplitude of the modulation : < 0.6%
Small, yet we account for that

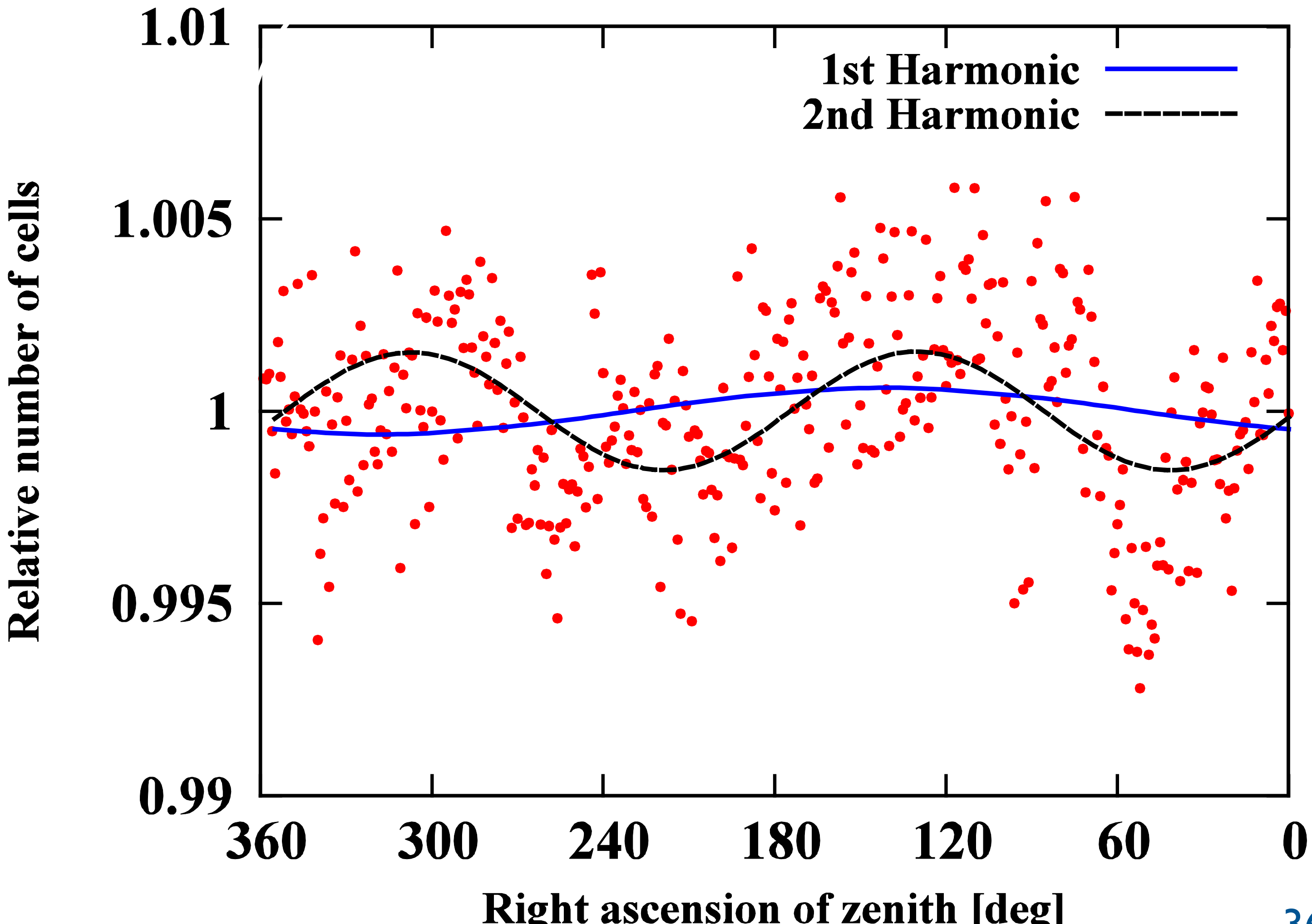

Large-scale analysis: sanity checks

First harmonic analysis in solar and antisidereal time
Evolution of the significance over time

First-harmonic amplitude in solar and anti-sidereal time not significant in any of the two energy bins

Energy	solar		anti-sidereal	
[EeV]	r_1	$P(\geq r_1)$	r_1	$P(\geq r_1)$
4 - 8	0.006	0.48	0.004	0.76
≥ 8	0.007	0.69	0.011	0.36

Significance of the first-harmonic amplitude in right ascension became larger as the exposure increased.
Cross-check with different fiducial cuts

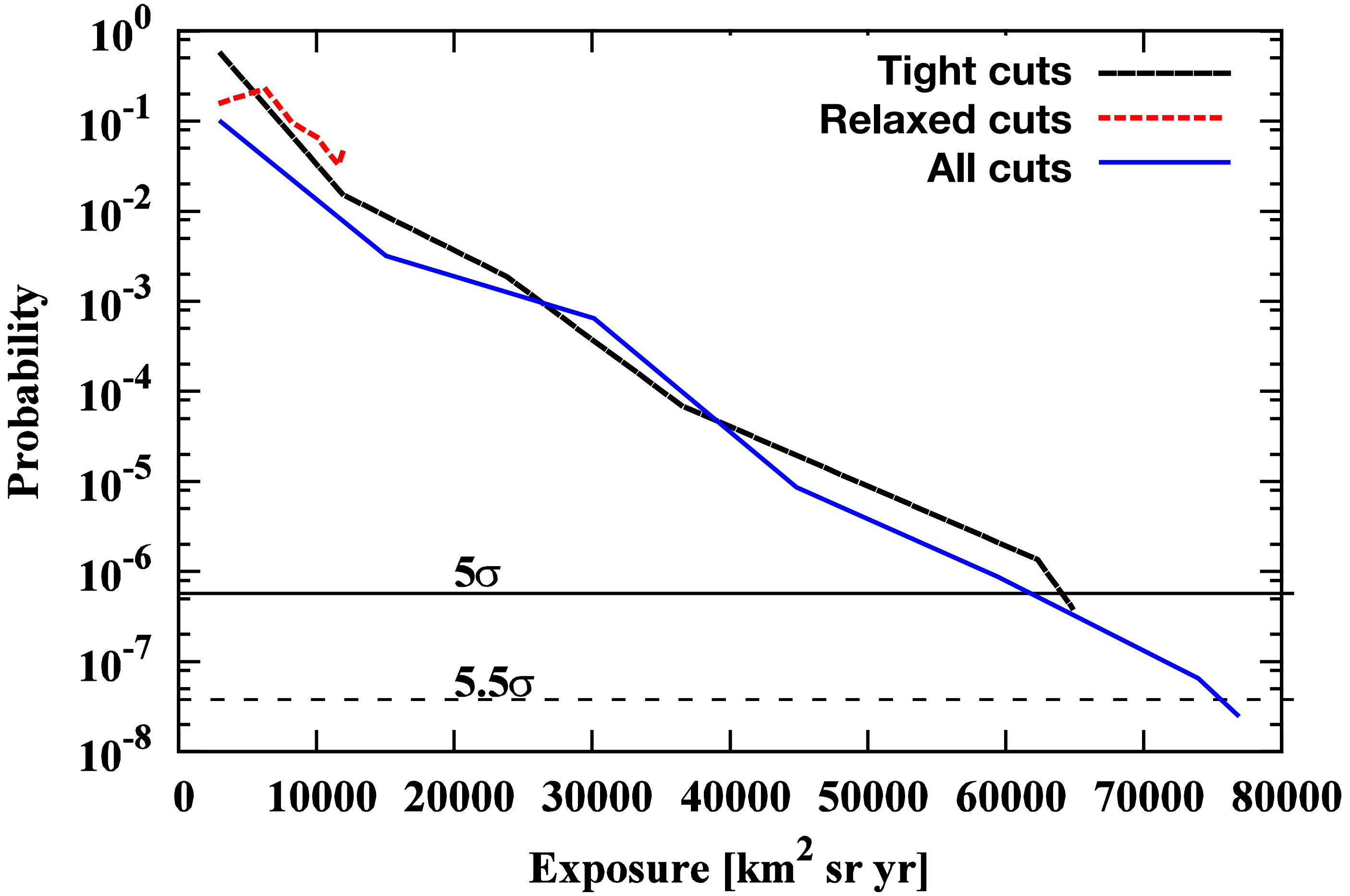

Auger alone: large-scale analysis

Method: Harmonic analysis in right ascension

[J. Linsley PRL 34 (1975) 1530]

Data corrected for atmospheric and geomagnetic effects

First-harmonic components

$$a_\alpha = \frac{2}{\mathcal{N}} \sum_{i=1}^{N} w_i \cos \alpha_i$$

$$b_\alpha = \frac{2}{\mathcal{N}} \sum_{i=1}^{N} w_i \sin \alpha_i$$

Modified to include weights w_i accounting for exposure variations and non-uniformities

Amplitude and phase

$$r_\alpha = \sqrt{a_\alpha^2 + b_\alpha^2}$$

$$\tan \varphi_\alpha = \frac{b_\alpha}{a_\alpha}$$

Chance probability for an amplitude being larger than that observed:

cumulative distribution function of the Rayleigh distribution

$$P(r_\alpha) = \exp(-\mathcal{N} r_\alpha^2 / 4)$$

Auger large-scale analysis: dipole reconstruction

Harmonic analysis in RA:

Only sensitive to the anisotropy component orthogonal to the Earth's rotation axis

The distribution of the azimuth angles is in turn sensitive to the N/S component:

Harmonic analysis in azimuthal angles performed

Under the assumption that the anisotropy is purely dipolar, the first-harmonic coefficients in RA and azimuth are sufficient to reconstruct the dipole

Reconstruction of amplitudes

$$d_\perp \approx \frac{r_\alpha}{\langle \cos \delta \rangle}$$

$$d_z \approx \frac{b_\varphi}{\cos \ell_{\rm obs} \langle \sin \theta \rangle}$$

Reconstruction of directions

$$\alpha_{\rm d} = \varphi_\alpha$$

$$\tan \delta_{\rm d} = \frac{d_z}{d_\perp}$$

Large-scale analysis: other studies

Second harmonic analysis applied in two energy bins (4-8 EeV and > 8 EeV)

[Auger Coll. arXiv 1808.03579, just accepted by ApJ]

		Harmonic	Components		Amplitude	Phase	Probability
Energy [EeV]	events	k	a_k^α	b_k^α	r_k^α	$\varphi_k^\alpha [°]$	$P(\geq r_k^\alpha)$
4 - 8	81,701	1	0.001 ± 0.005	0.005 ± 0.005	0.005	80 ± 60	0.60
		2	-0.001 ± 0.005	0.001 ± 0.005	0.002	70 ± 80	0.94
≥ 8	32,187	1	-0.008 ± 0.008	0.046 ± 0.008	0.047	100 ± 10	2.6×10^{-8}
		2	0.013 ± 0.008	0.012 ± 0.008	0.018	21 ± 12	0.065

No statistically significant second harmonic in any of the two energy bin

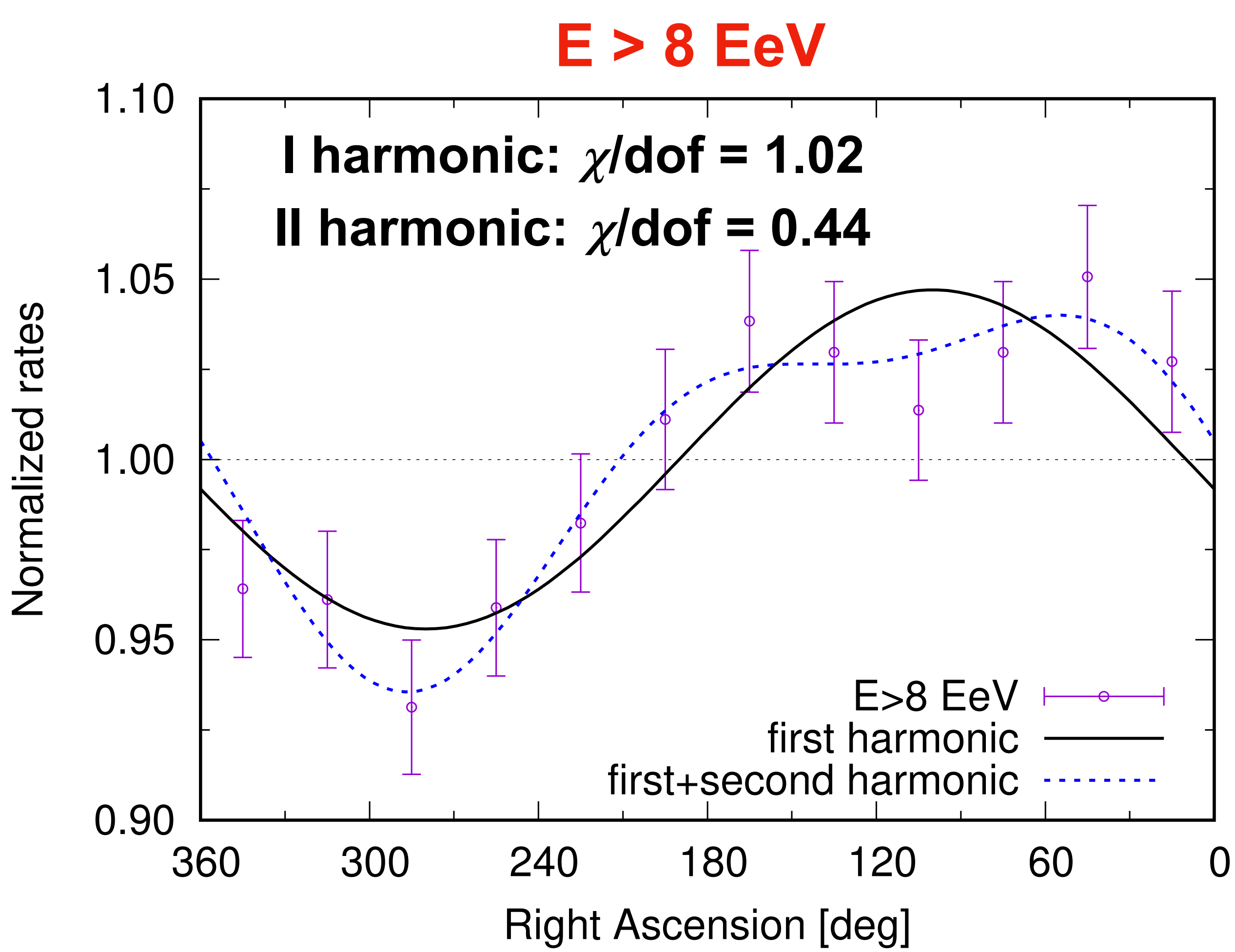

Large-scale analysis: other studies

Study of a possible evolution of the first harmonic in RA vs energy

[Auger Coll. arXiv 1808.03579, just accepted by ApJ]

Dividing the E > 8 EeV bin into three

Energy [EeV]	events	a_1^α	b_1^α	r_1^α	φ_1^α [°]	$P(\geq r_1^\alpha)$
8 - 16	24,070	-0.011 ± 0.009	0.044 ± 0.009	0.046	104 ± 11	3.7×10^{-6}
16 - 32	6,604	0.007 ± 0.017	0.050 ± 0.017	0.051	82 ± 20	0.014
≥ 32	1,513	-0.03 ± 0.04	0.05 ± 0.04	0.06	115 ± 35	0.26

Constant phase in spite of a (naturally) more limited significance of the amplitude

Dipole amplitude reconstruction

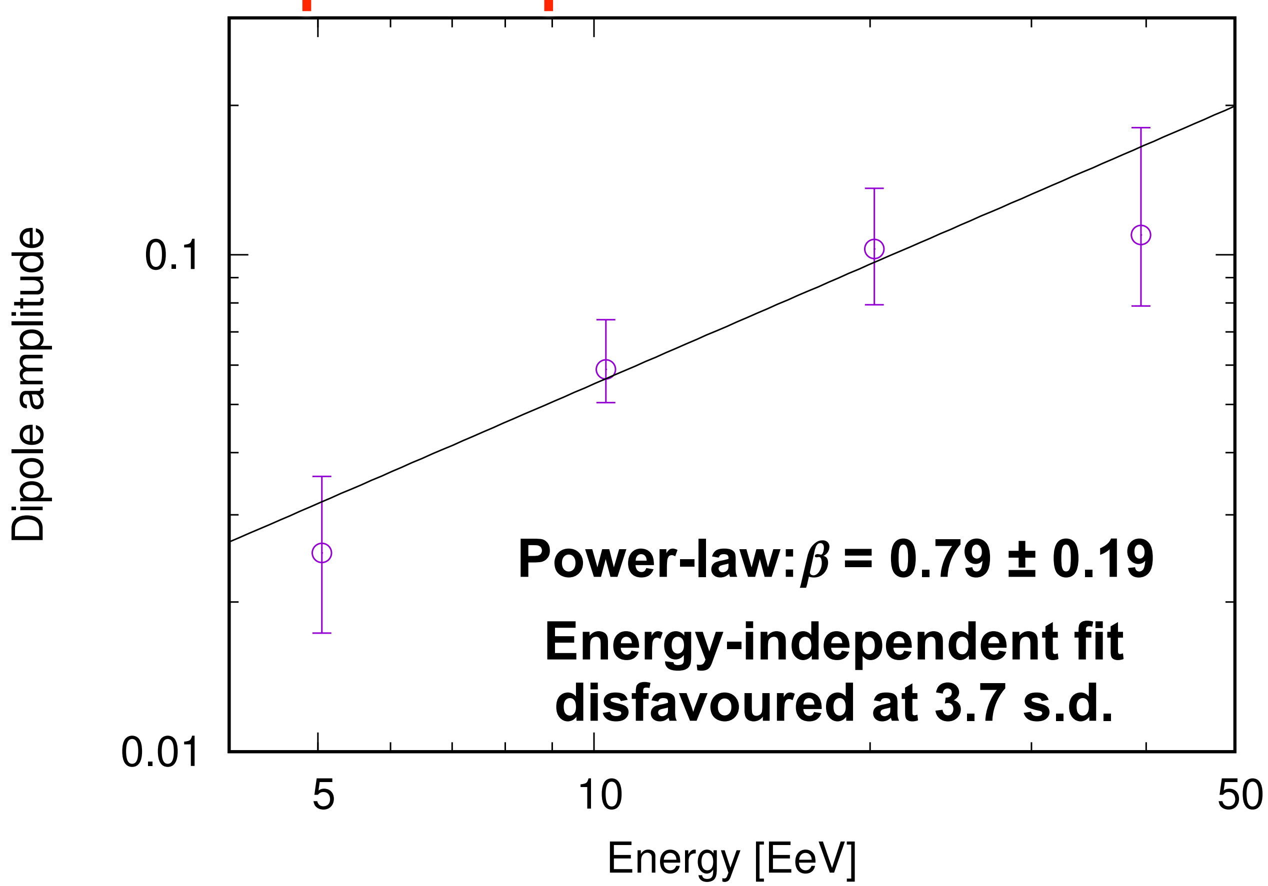

Indication of an increase of the dipole amplitude vs energy

Constant direction

Auger "small"-scale analysis:"close-by" galaxies

The candidate galaxies and the analysis method

[Auger Coll. ApJL 853 (2018) L29]

γ-ray AGNs from the 2FHL catalog

(Fermi-LAT, E>50 GeV)

R < 250 Mpc

17 objects (among which Cen A, M87, Mkn 421, Mkn501…)

γ-ray flux used as proxy for the UHECR flux

γ-ray SBGs searched by Fermi-LAT

(from the HCN survey)

R < 250 Mpc

Radio-flux > 0.3 Jy

23 objects (among which M82, NGC253, and other 5 detected in γ)

Radio-flux used as proxy for the UHECR flux

Method: Unbinned maximum LH analysis

UHECR sky model: isotropy + anisotropic component from the sources

Directional exposure accounted

TS = LH ratio between H(UHECR sky model) and H(isotropy)

TS maximised vs search radius, ϑ, and anisotropic fraction, α

Test repeated over several energy thresholds (E > 20 EeV, up to E > 80 EeV, 1 EeV steps)

Flux attenuation accounted for at each energy threshold

Composition inferred by Auger data accounted for

“Small”-scale analysis: other source models

Flux-limited samples of extra-galactic sources
[Auger Coll. ApJL 853 (2018) L29]

2MRS (infrared)
TS is maximum for E > 38 EeV
α = 7 ± 4%, ϑ = 12° ± 6°
Post-trial (2 par. and E scan): 2.7 s.d.

Swift-BAT (X-rays)
TS is maximum for E > 39 EeV
α = 16 ± 8%, ϑ = 13° ± 7°
Post-trial (2 par. and E scan): 3.2 s.d.

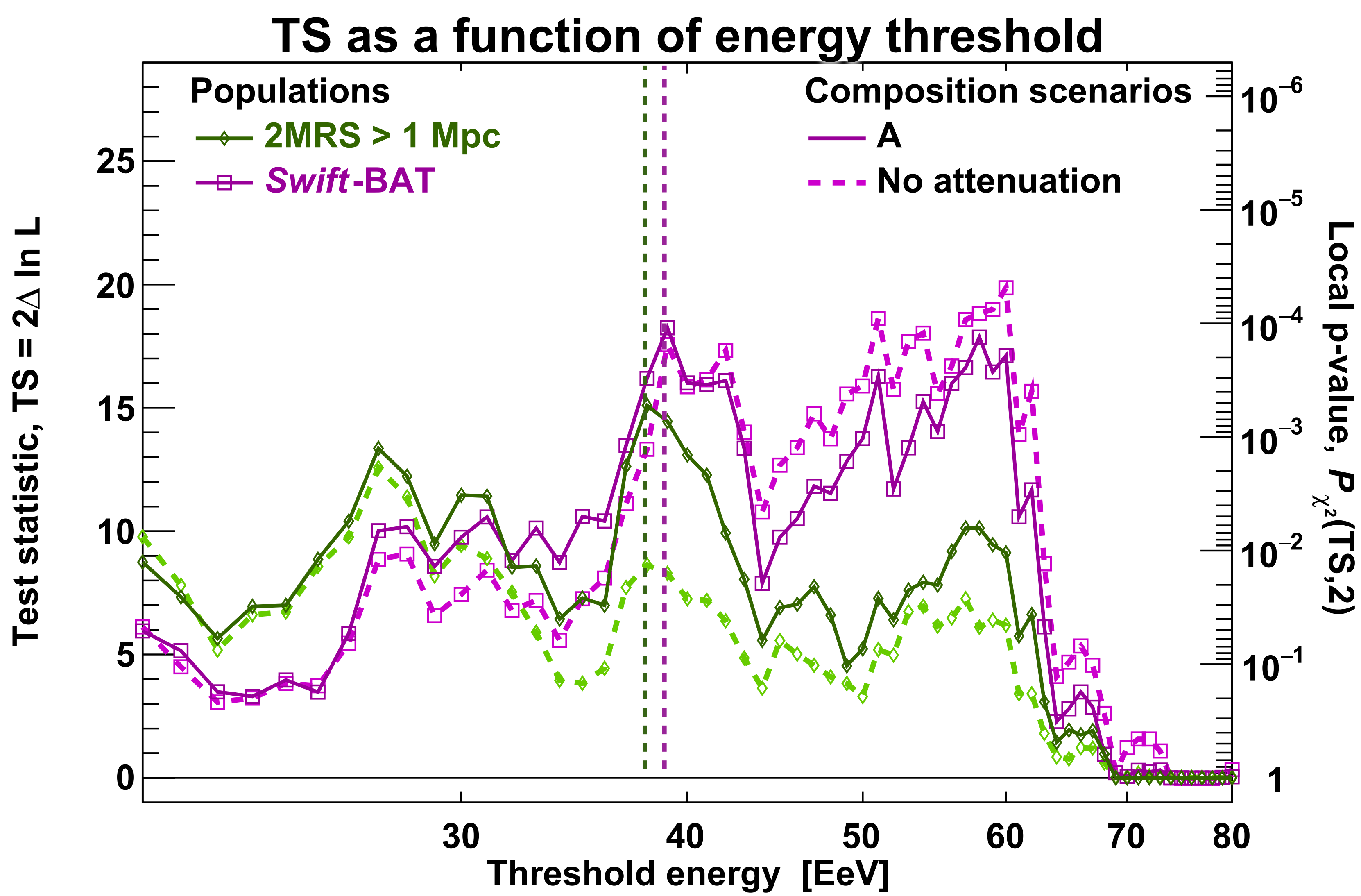

The contribution of SBGs to the indication of anisotropy remains larger than that of alternative catalogs tested

Harmonic analysis vs energy

Splitting the E>8 bin in three

Auger Coll. arXiv 1808.03579, just accepted by ApJ]

Right ascension

Energy [EeV]	events	a_1^α	b_1^α	r_1^α	φ_1^α [°]	$P(\geq r_1^\alpha)$
8 - 16	24,070	-0.011 ± 0.009	0.044 ± 0.009	0.046	104 ± 11	3.7×10^{-6}
16 - 32	6,604	0.007 ± 0.017	0.050 ± 0.017	0.051	82 ± 20	0.014
≥ 32	1,513	-0.03 ± 0.04	0.05 ± 0.04	0.06	115 ± 35	0.26

Azimuth

Energy [EeV]	a_1^ϕ	b_1^ϕ	$P(\geq \|a_1^\phi\|)$	$P(\geq \|b_1^\phi\|)$
8 - 16	-0.013 ± 0.009	-0.004 ± 0.009	0.15	0.66
16 - 32	0.003 ± 0.017	-0.042 ± 0.017	0.86	0.013
≥ 32	0.05 ± 0.04	-0.04 ± 0.04	0.21	0.32

Dipole reconstruction vs energy

[Auger Coll. arXiv 1808.03579, just accepted by ApJ]

Energy [EeV] interval	median	$d_\perp$	d_z	d	α_d [°]	δ_d [°]
4 - 8	5.0	$0.006^{+0.007}_{-0.003}$	-0.024 ± 0.009	$0.025^{+0.010}_{-0.007}$	80 ± 60	-75^{+17}_{-8}
≥ 8	11.5	$0.060^{+0.011}_{-0.010}$	-0.026 ± 0.015	$0.065^{+0.013}_{-0.009}$	100 ± 10	-24^{+12}_{-13}
8 - 16	10.3	$0.058^{+0.013}_{-0.011}$	-0.008 ± 0.017	$0.059^{+0.015}_{-0.008}$	104 ± 11	-8^{+16}_{-16}
16 - 32	20.2	$0.065^{+0.025}_{-0.018}$	-0.08 ± 0.03	$0.10^{+0.03}_{-0.02}$	82 ± 20	-50^{+15}_{-14}
≥ 32	39.5	$0.08^{+0.05}_{-0.03}$	-0.08 ± 0.07	$0.11^{+0.07}_{-0.03}$	115 ± 35	-46^{+28}_{-26}

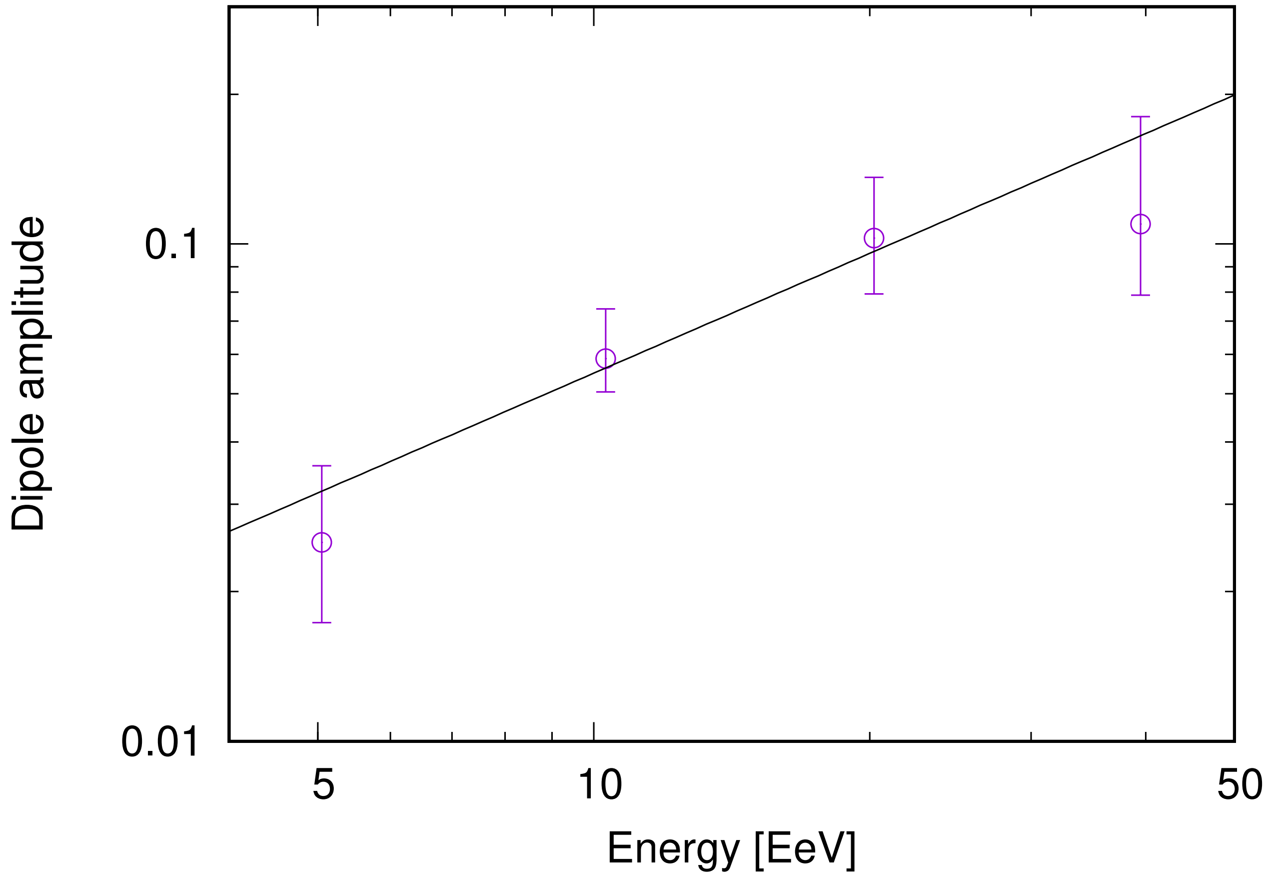

Maximum likelihood fit

Power-law index β = 0.79 ± 0.19

Energy-independent fit disfavoured at 3.7 s.d.

Reconstruction of dipole + quadrupole

[Auger Coll. arXiv 1808.03579, just accepted by ApJ]

Energy [EeV]	d_i	Q_{ij}
4 - 8	$d_x = -0.005 \pm 0.008$	$Q_{zz} = -0.01 \pm 0.04$
	$d_y = 0.005 \pm 0.008$	$Q_{xx} - Q_{yy} = -0.007 \pm 0.029$
	$d_z = -0.032 \pm 0.024$	$Q_{xy} = 0.004 \pm 0.015$
		$Q_{xz} = -0.020 \pm 0.019$
		$Q_{yz} = -0.005 \pm 0.019$
≥ 8	$d_x = -0.003 \pm 0.013$	$Q_{zz} = 0.02 \pm 0.06$
	$d_y = 0.050 \pm 0.013$	$Q_{xx} - Q_{yy} = 0.08 \pm 0.05$
	$d_z = -0.02 \pm 0.04$	$Q_{xy} = 0.038 \pm 0.024$
		$Q_{xz} = 0.02 \pm 0.03$
		$Q_{yz} = -0.03 \pm 0.03$

None of the quadrupole components is statistically significant

Reconstructed dipole consistent with those obtained under the pure-dipole assumption